Electrophoresis-assisted multilayer assembly of nanoparticles for sensitive lateral flow immunoassay

Vasily G. Panferov,[a,b,c] Nikita A. Ivanov, [a,b] Tony Mazzulli,[d] Davor Brinc,[e] Vathany Kulasingam,[e] and Sergey N. Krylov*[a,b]

[a]   Dr. V. G. Panferov, N. A. Ivanov, Prof. S. N. Krylov
        Department of Chemistry, York University, 4700 Keele Street, Toronto, Ontario M3J 1P3, Canada
        E-mails: vpanf@yorku.ca, nivanov@yorku.ca, skrylov@yorku.ca
[b]   Dr. V. G. Panferov, N. A. Ivanov, Prof. S. N. Krylov
        Centre for Research on Biomolecular Interactions, York University, 4700 Keele Street, Toronto, Ontario M3J 1P3, Canada
[c]   Dr. V. G. Panferov
        A.N. Bach Institute of Biochemistry, Federal Research Centre "Fundamentals of Biotechnology" Russian Academy of Sciences, 33 Leninsky Prospect, Moscow 119071, Russia
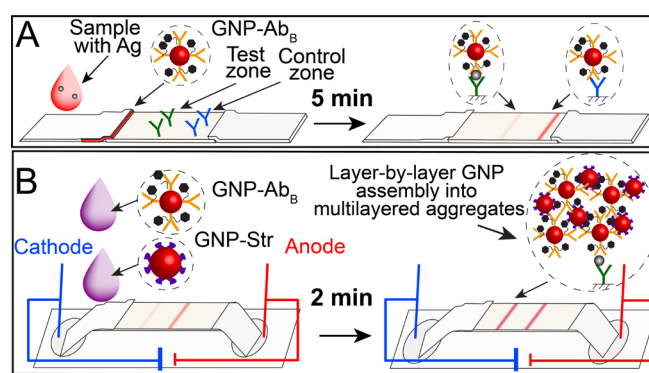[d]   Dr. Tony Mazzulli, Sinai Health, Toronto, 600 University Avenue, Toronto, Ontario M5G 1X5, Canada
        E-mail: tony.mazzulli@sinaihealth.ca
[e]   Dr. Davor Brinc, Dr. Vathany Kulasingam
        Toronto General Hospital: University Health Network, 200 Elizabeth St., Toronto, Ontario M5G 2C4, Canada
        E-mails: davor.brinc@uhn.ca, dr.vathany.kulasingam@uhn.ca

Abstract: Lateral flow immunoassay (LFIA) is a rapid, simple, and inexpensive method for point-of-need analysis. A major limitation of LFIA is a high limit of detection (LOD), which impacts its diagnostic sensitivity. To overcome this limitation, we introduce a signal-enhancement procedure that is performed after completing LFIA and involves controllably moving biotin- and streptavidin-functionalized gold nanoparticles along the test strip by electrophoresis. The nanoparticles link to immunocomplexes and each other forming multilayer aggregates on the test strip, thus, enhancing the signal. Here, we demonstrate lowering the LOD of hepatitis B surface antigen from approximately 8 to 0.12 ng/mL, making it clinically acceptable. Testing 76 clinical samples of serum and plasma for hepatitis B revealed that signal enhancement increased diagnostic sensitivity of LFIA from 72% to 98% while not affecting its 90% specificity. Electrophoresis-driven detection enhancement of LFIA is universal (antigen-independent), takes two minutes, and can be performed by an untrained person using an inexpensive accessory.

Figure 1. Schematic depiction of: **(A)** conventional LFIA and **(B)** enhancement step performed after completion of LFIA by means of electrophoretically-assisted layer-by-layer assembly of gold nanoparticles (GNPs). Ag is antigen in the sample. Yellow Y (Ab$_B$) is biotinylated second antibody against Ag. Green Y is first antibody against Ag; it is immobilized in the test zone. Blue Y is anti-species antibody, which is immobilized in the control zone.

Point-of-need detection methods benefit medical testing, food-quality control, and environmental monitoring.[1,2] Lateral flow immunoassay (LFIA) is a rapid, simple, and inexpensive molecular detection method which can be used for medical testing by primary care providers.[3] LFIA utilizes test strips: preassembled overlapping membranes loaded with dried immunoreagents (several types of antibodies). A drop of the liquid sample containing an antigen to be detected is placed on the strip, and capillary forces move it along the membranes. The migration of the liquid sample through the zones of dried immunoreagents causes the rehydration of the latter and facilitates affinity binding of a labeled antibody to the antigen. This binding leads to the formation of a colored zone with a labeled immunocomplex on the strip.[4] A qualitative result is obtained within 5–15 min by visually examining the test strip for the presence and/or absence of two (or more) colored zones (Figure 1A).

The major tradeoff for simplicity, rapidness, and low cost of LFIA is a relatively high limit of detection (LOD). The high LOD restricts LFIA application only to a small set of clinically-important disease biomarkers and pathogens.[5] Reducing the LOD of LFIA is an important task that attracts growing interest of the research community.[6,7] The LOD of LFIA cannot be lowered without compromising to some extent one or more of the three key benefits of conventional LFIA: simplicity, rapidness, and low cost. An acceptable compromise is the one that does not prevent the

use of enhanced LFIA by an untrained analyst at the points of need. Moreover, to justify any LOD-lowering modification, the level of reduction should be sufficient to facilitate the detection of clinically-relevant concentrations.

Multiple strategies for lowering LOD in LFIA aim at the amplification of the signal from immunocomplexes by increasing the label amount per complex. Such increase may be achieved by crosslinking functionalized nanoparticles (conjugates), where the primary conjugate reacts with the antigen, and the secondary conjugate binds to the primary one, resulting in the accumulation of a high amount of the label per immunocomplex. This strategy of signal amplification is utilized in various bioanalytical methods such as ELISA, immunohistochemistry, and biosensing.[8,9] All these methods use consequent delivery of reagents and require multiple incubation and washing steps. Keeping LFIA within the paradigm of a method driven by capillary action makes this multi-step strategy inapplicable. When the membrane is wetted by sample loading, capillary-action-driven mass transfer along the membrane becomes negligible. Because of this limitation, primary and secondary conjugates are usually loaded at once along with the sample. As a result, conjugates crosslink to each other before reaching the immunocomplex-forming-zone (the test zone with antibodies). Such uncontrollable crosslinking leads to the formation of micrometer-sized aggregates non-specifically

retained by the membrane, resulting in high background and affecting achievable LOD reduction.[10]

To overcome the limitation imposed by capillary-action-driven mass transfer, we propose electrophoresis as a driving force of controllable conjugate migration (Figure 1B). The use of electrophoresis-assisted migration allows multiple deliveries of the conjugates to the test zone on a wet strip after performing conventional LFIA.

While setting up this proof-of-principle study, we aimed to adhere to the standard strip geometry, the standard sandwich format of the assay, and the conventional spherical-shape gold nanoparticles (GNP) as labels. This way, our LOD lowering strategy could be quickly optimized and adopted for practical use if proven effective. We also aimed to make electrophoresis-enhanced detection a simple procedure utilizing identical conditions for migration of primary and secondary conjugates and excluding washing and/or incubation steps.

Electrophoresis constitutes an *a priori* very simple way of consequent delivery of primary and secondary conjugates to the test zone. It is somewhat counterintuitive that this approach has not been utilized for controlled complex assembly in LFIA yet. Only capillary-action-driven migration of a mixture of low-concentration functionalized GNPs has been used for LFIA, resulting in a 3 to 30-fold decrease in LOD.[10-12] Alternatively, multilayer assembly of GNP through host-guest recognition on the test strip was demonstrated through a time-consuming and cumbersome procedure of incubating the test strip with the reagents and washing it after each assembly cycle.[13] We hypothesize that the consequent delivery of GNP conjugates by electrophoresis would allow us to (*i*) eliminate the non-specific formation of large aggregates and, thus, reduce the background, (*ii*) include a higher number of labels in immunocomplexes, hence, providing higher signal, and (*iii*) perform one-step post-assay signal amplification with minimal user involvement. Cumulatively, reducing the background and increasing the signal should reduce the LOD.

The proposed enhancement approach is schematically depicted in Figure 1B. Notably, the enhancement step is used only if LFIA results are negative or low positive. In such a case, the terminals of the membrane are immersed into two reservoirs containing the electrolyte and electrodes. As GNPs are negatively charged, the cathode is at the loading terminus of the membrane. The voltage is applied, and a drop of GNP-streptavidin conjugate (GNP-Str) is loaded first, followed by GNP conjugated with biotinylated second antibody (GNP-Ab$_B$) and so on. Note that GNP-Ab$_B$ should be used in conventional LFIA (Figure 1A) to label the antigen in the test zone. Each of the two GNP conjugates is moved electrophoretically to the anode terminus of the membrane. The conjugate reacts in the test zone with preassembled sandwich immunocomplexes (Ab:Ag:GNP-Ab$_B$), forming the multilayer aggregates. The excess of unreacted GNP conjugates is moved electrophoretically beyond the test zone. Having the concept explained, we can move to the description of results in four-step method development.

First, we synthesized and characterized GNP, GNP-Ab$_B$, and GNP-Str (Figure S1). The synthesized GNP (22.7 ± 1.9 nm in size with an elongation coefficient of 1.12 ± 0.07) and its conjugates were stable; no aggregates were detected during their preparation (Figure S2). The affine capturing of conjugates on the membranes confirmed the retained binding activity of the proteins immobilized on GNP (Figure S3).
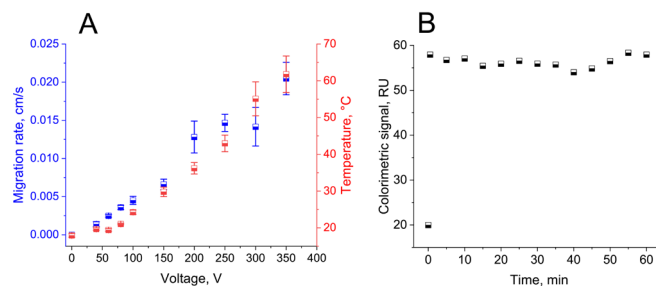
Figure 2. **(A)** The effect of voltage on the conjugate migration rate and test strip temperature. **(B)** The stability of immunocomplexes at 200 V applied to the test strip.

Second, we optimized conditions to provide the lowest LOD for conventional LFIA *via* selecting an optimum combination of monoclonal antibodies (Figure S4). Conventional LFIA utilizes two monoclonal antibodies binding to different epitopes of Ag (Figure 1A). The first antibody is immobilized in the test zone, and the second antibody (GNP-Ab$_B$) is deposited in the conjugate-storage zone and can be mobilized when the liquid sample moves through this zone. A control zone had an immobilized antibody against the second antibody. The only minor deviation from conventional LFIA was that the second antibody was biotinylated to facilitate GNP-Str linking in the signal enhancement. As an antigen, we used hepatitis B surface antigen (HBsAg). Below, we use "Ag" for both general notation for antigen and specific antigen used in this study. As a liquid sample, we used human serum spiked with Ag in the method-development part of this study (plasma and serum of patients were used in the utility-demonstration part).

Third, we optimized conditions for electrophoresis and evaluated its ability to facilitate migration of GNP conjugates to the test zone. We studied various electrolyte compositions (Table S1, Figure S5) and selected 50 mM sodium borate, pH 8.1, supplemented with 0.05% 2-hydroxyethyl cellulose (MW = 380 kDa) and 0.08% sodium dodecyl sulfate. The selected electrolyte ensures low Joule heating because its low conductivity.[14] The optimization of the test-strip holder geometry (type and positions of electrodes and volumes of reservoirs) was also performed, and conditions supporting continuous stable electrophoresis (Figure S6) were used in this study.

The conjugate migration rate (R^2 = 0.962) and temperature (R^2 = 0.960) of nitrocellulose membrane show near linear dependencies on the voltage applied (Figure 2A). We chose 200 V for further development as it facilitates fast migration of GNP conjugates while eliminating the risks of denaturing the antibodies and antigen due to temperature increase by Joule heating (temperature of the test strip was below 40°C). We confirmed that the formed immucomplexes (Ab:Ag:GNP-Ab$_B$:GNP-Str)$_n$ did not show dissociation even after 1-h of applying 200 V to the test strip (Figure 2B).

Fourth, the optimized conditions were used to evaluate multiple deliveries of GNP conjugates to the test zone. We observed the narrowing of the applied conjugate bands leading to their increased coloration at the beginning of the electrophoresis-assisted migration (Figure 3A). The narrowing is caused by electrostacking of GNP conjugates on the interface of the diluted conjugate buffer (a zone with a higher electric field) and a more concentrated electrolyte (a zone with lower electric field).[15]

Based on the spatial profiles of the color intensity, we used the position with the highest stacking of the conjugates (blue
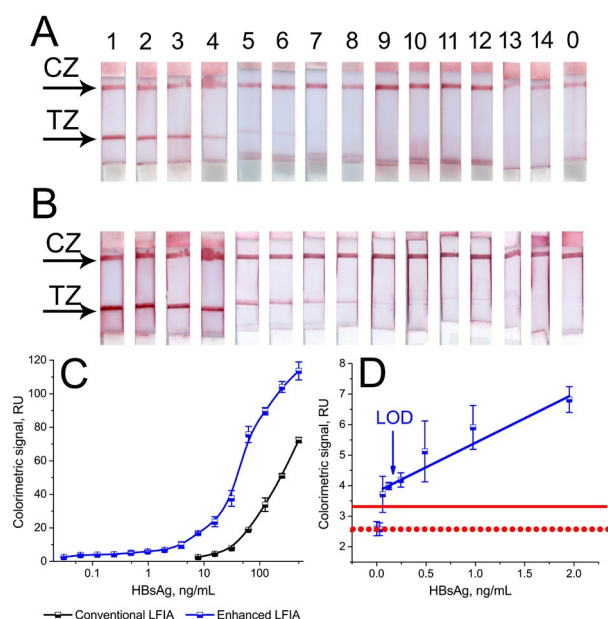
2
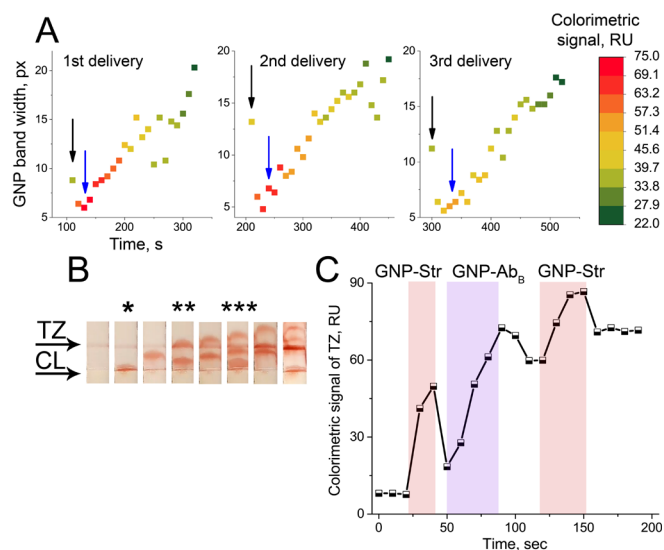
Figure 3. Electrophoretically-assisted multiple passages of GNP conjugates. **(A)** The widths and colorimetric signal intensities of the bands migrating through the strip upon three consecutive loads of GNP-Str. Black arrows show the injection of GNP-Str; blue arrows show the selected position of test zone. **(B)** Progressive images (from left to right) of a test strip after LFIA of 30 ng/mL HBsAg and upon three consecutive additions of GNP conjugates. The addition of conjugates is marked with asterisks: GNP-Str (*), GNP-Ab$_B$ (**), and GNP-Str (***). Conjugate loading (CL) zone is shown with the arrow. **(C)** The dependence of color intensity in the test zone (shown in panel B) in the course of multilayer assembly. The migration of the conjugates through the test zone is depicted by the red (GNP-Str) and violet (GNP-Ab$_B$) rectangles.

Figure 4. LFIA of varying concentrations of HBsAg spiked into human serum. Images of test strips for: **(A)** conventional LFIA and **(B)** enhanced LFIA. The numbers above the test-strip images correspond to concentrations of HBsAg in ng/mL: 1 – 500, 2 – 250, 3 – 125, 4 – 62.5, 5 – 31.2, 6 – 15.6, 7 – 7.8, 8 – 3.9, 9 – 1.9, 10 – 0.98, 11 – 0.49, 12 – 0.244, 13 – 0.122, 14 – 0.06, and 0 – blank. **(C)** Semilogarithmic calibration plot for conventional LFIA (black) and enhanced LFIA (blue) for the full range of HBsAg concentrations. **(D)** Linear calibration plot (blue) for enhanced LFIA for low concentrations of HBsAg. The red dotted line shows the background of blank while the solid red line shows the background plus three standard deviations The blue arrow indicates the LOD value.

arrows in Figure 3A) to place the test zone. We then evaluated layer-by-layer assembly for colorimetric signal enhancement. We used a test strip with a faintly-colored test zone containing the sandwich complexes (Ab:Ag:GNP-Ab$_B$) (Figure 3B). GNP-Str and GNP-Ab$_B$ were consequently moved by electrophoresis through the test zone to facilitate the assembly of the multilayer aggregates (Ab:Ag:GNP-Ab$_B$:[GNP-Str:GNP-Ab$_B$]$_n$) (Figure 3C, the passage of the conjugate is indicated with colored rectangles). Electrophoresis also facilitated the seamless washing step in which the excess of unreacted conjugates was moved from the test zone to the anode reservoir. Limiting the number of conjugate loads to four facilitated the optimum balance between signal enhancement and background coloration caused by non-specific adsorption of conjugate particles in the test zone.

In summary, by using the electrophoresis as a driving force, we performed the consequent delivery of multiple GNP conjugates to the test zone. As a result, we achieved layer-by-layer assembly of GNPs into multilayer aggregates in the test zone, where individual GNPs are linked to the immunocomplexes and each other via the streptavidin-biotin bridge.

Having the method established, we evaluated the degree of LOD reduction by using the developed approach. The Ag was spiked in human serum at concentrations ranging from 0.03 to 500 ng/mL. The LOD of the conventional LFIA was equal to 7.8 ng/mL (test strip 7, Figure 4A). The coloration of the test zone for non-spiked serum was not observed, confirming high specificity of the assay. However, the LOD value in the conventional LFIA in this study did not meet the clinical requirement for early-stage diagnostics of hepatitis B set by the World Health Organization (WHO, the required LOD is 0.13 IU/mL, based on 1 IU/mL = 1–10 ng/mL),[16] and the USA Food and Drug Administration (FDA, the required LOD is 0.5 ng/mL).[17]

We then performed our enhancement procedure using the same test strips. Electrophoresis-assisted layer-by-layer assembly of GNP into multilayer aggregates resulted in a significant increase of the colorimetric signal, providing visually-detectable coloration of previously undetectable test zones (test strips 8 to 13 in Figure 4B). The LOD of enhanced LFIA was 0.12 ng/mL (test strip 13, Figure 4B), thus facilitating detection enhancement by more than 60 times (Figure 4C). We observed some coloration of the test zone for the non-spiked serum (background of enhanced LFIA, Figure 4D). This coloration may be explained by the non-specific adsorption of conjugates during the enhancement procedure. The colorimetric signal from the Ag-free serum was low and did not interfere with the visual detection. (Figure 4D). Further optimization of LFIA conditions may reduce non-specific adsorption and facilitate even lower LOD values. The achieved LOD meets requirements set by both WHO and FDA and facilitates diagnostics at the early stages of hepatitis B infection.

The developed layer-by-layer GNP assembly provides the highest reduction of LOD (more than 60 times) as compared to conventionally used biotin-streptavidin aggregation of nanoparticles in mixtures (2–30 times) (Table S2). The comparison of the absolute LOD values reported in other articles cannot be conclusive because assays have been performed under different LFIA conditions: affinity of antibodies, types of membrane, size of GNP, etc. The LOD of our enhanced LFIA meets clinically-relevant concentrations for hepatitis B for point-of-care diagnostics (Table S3). Our enhanced LFIA showed the linear range (R^2 = 0.994) within 0.12–62.5 ng/mL of the Ag (Figure S7), corresponding to the clinically-significant range for this Ag. Using 20 healthy serum samples spiked with known
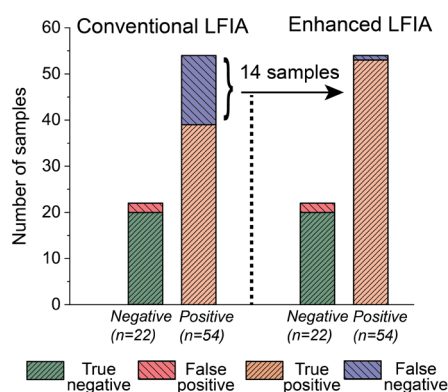
Figure 5. Results of conventional and enhanced LFIA of serum and plasma samples from healthy (n = 22) and hepatitis B infected (n = 54) patients.

concentrations of Ag, we confirmed high-accuracy (R^2 = 0.979) of enhanced LFIA (Figure S8).

Then, enhanced LFIA was used in the analyses of clinical samples: 57 serum and 19 plasma samples from both infected and healthy patients (Figure 5). Before being analyzed by LFIA, these samples were subjected to Abbott chemiluminescent microparticle immunoassay Alinity I for the hepatitis B antigen by Abbott Laboratories performed in laboratories of two hospitals (HBsAg 08P08 quantitative assay, reactive: $\geq$ 0.05 IU/mL, Alinity I, Abbott Diagnostics, Abbott Park, IL, USA). Twenty-two samples were identified as negative (healthy), and the remaining fifty-four were positive in the Abbot I assay (Table S4, Figure S9). We used the results of this chemiluminescent immunoassay as a reference in the determination of the sensitivity and specificity of our LFIA.

Conventional LFIA was performed first. Conventional LFIA recognized two samples as positive (false-positive result for samples #2 and #14, Figure S9) and twenty as negative, which gave a specificity of 90%. It showed 15 false negative results out of 54 true positive samples, thus facilitating sensitivity of approximately 72%.

The enhancement procedure was performed for samples showing no coloration of the test zone or coloration below 4 RU. The enhanced LFIA demonstrated the same specificity of approximately 90% (2 false positive out of 22 true negative) as the conventional LFIA (Figure 5). It showed coloration of the test zone for low positive samples, giving a single false negative result for the 54 true positive samples and raising assay sensitivity to 98% (Figure 5, Figure S9). We thus confirmed that the enhancement procedure maintains specificity comparable to conventional LFIA while facilitating much higher sensitivity for the detection of clinically-relevant concentrations of the hepatitis B Ag in real samples.

At least one-week storage of test strips after performing conventional LFIA did not influence the efficiency of enhancement. Thus, the assay may be performed in two stages – the first stage is conventional LFIA performed at point-of-need, and the second stage is the enhancement procedure performed for negative/low positive samples in a lab environment (Figure S10). Such a two-stage assay may significantly reduce the workload of hospital testing facilities and facilitate more affordable diagnostics in resource-limited settings.

We also performed preliminary experiments for the detection of this Ag in the whole capillary blood. Collection of capillary blood is less traumatic than a collection of vein blood. Capillary blood is used for the screening of newborns, which is a routine procedure

if the mother is infected with hepatitis B. Our preliminary results confirm the applicability of the enhanced LFIA for the detection of hepatitis B Ag in whole capillary blood (Figure S11). In general, the visual detection of red-colored GNP is hindered in whole blood samples as blood is also red-colored. Advantageously, electrophoresis facilitates the migration of the colored components of the blood beyond the test zone and the electrokinetic washing of the test strip. As a result, a lower background staining of the strip after the assay was observed, facilitating more convenient visual detection for LFIA in colored samples, such as whole blood.

Although electrophoresis-assisted migration was used to enhance point-of-need methods[18-23] and LFIA[24-29], there were no reports of the highly enabling combination of electrophoretic migration and nanoparticle assembly into multilayer aggregates. In the previous reports, the enhancement was achieved either by preconcentration,[30,31] or via the creation of more favorable conditions for affine binding,[32] *i.e.*, enhancement was "analyte-focused". The previously reported enhancement methods were applicable only to particular antigens (*e.g.*, isotachophoresis conditions for a given molecule cannot be used for another one without re-optimization), and, thus, cannot be easily adapted for other antigens of interest. Even if nanoparticles were used, they acted as a label similar to the conventional assay, and their unique property of facilitating the multilayer assembly was not utilized. In this work, for the first time, electrophoresis was used to facilitate effective nanoparticle crosslinking on the test strip. Focusing on nanoparticles (acting as labels) rather than on the analyte makes the approach analyte-independent and easily adaptable for practical use. The electrophoresis-assisted reagent delivery may be adopted for other post-assay enhancement strategies as all of them require reagent delivery on a wet test strip.[6,7]

Implementing the LFIA enhancement strategy proposed here requires additional accessories (a power supply and a strip holder) and an additional assay step (adding conjugates). In the lab environment, power supplies are routinely used for gel electrophoresis;, thus, the reported technology may be directly adopted without modifications. Portable power supplies may facilitate this assay in a non-lab setting.[29] As for the holder, in this work, it was fabricated from poly(methyl methacrylate) using a milling machine. However, it can be mass-produced, *e.g.*, by injection molding or material casting. The holder is the only accessory; it does not require maintenance and can be used by an untrained person. The holder is inexpensive (Table S5) and may be used for a large number of assays (we performed more than 1000 electrophoresis-assisted assays using a single holder). As for the conjugates, we implemented GNP-Ab as the antigen-capturing conjugate and biotin/streptavidin-functionalized GNP for multilayer assembly. Because electrophoresis is a universal method for charged-particle migration, the reported strategy may be easily adapted for various affine binders,[33] and nanoparticles.[34] Moreover, to achieve lower LOD values, this strategy may be combined with various signal detection approaches. First, electrophoresis is used for the accumulation of a higher number of labels. Second, the accumulated labels are registered with a more sensitive than bare-eye signal detection method,[35] *e.g.*, Raman spectroscopy,[36] thermal contrast,[37] and electrochemiluminescence.[38]

To summarize, the developed post-assay enhancement of conventional LFIA utilizes the combination of two fundamental

principles: electrophoresis of functionalized GNP and their assembly into aggregates. Thus, the enhancement is universal and easily adaptable to various antigens. We believe that the reported electrophoresis-assisted LFIA will contribute to the field of point-of-need assays and further will be applied for other post-assay enhancement procedures.

Acknowledgements

Keywords: Electrophoresis; Lateral-flow immunoassay; Layer-by-layer assembly of gold nanoparticles; Limit of detection; Point-of-care detection.

Data availability statement

The raw data and figures that support the findings of this study are openly available in "Figshare" at

https://doi.org/10.6084/m9.figshare.20124224.v1

References

[1] J. Qin, W. Wang, L. Gao, S. Q. Yao, *Chem. Sci.* **2022**, *13*, 2857–2876.

[2] W. Feng, A. M. Newbigging, C. Le, B. Pang, H. Peng, Y. Cao, J. Wu, G. Abbas, J. Song, D.-B. Wang, M. Cui, J. Tao, D. L. Tyrrell, X.-E. Zhang, H. Zhang, X. C. Le, *Anal. Chem.* **2020**, 92, 10196–10209..

[3] Y. Zhou, Y. Wu, L. Ding, X. Huang, Y. Xiong, *TrAC Trends Anal. Chem.* **2021**, *145*, 116452.

[4] G. A. Posthuma-Trumpie, J. Korf, A. van Amerongen, *Anal. Bioanal. Chem.* **2009**, *393*, 569–582.

[5] Y. Liu, L. Zhan, Z. Qin, J. Sackrison, J. C. Bischof, *ACS Nano* **2021**, *15*, 3593–3611.

[6] J. D. Bishop, H. V. Hsieh, D. J. Gasperino, B. H. Weigl, *Lab Chip* **2019**, *19*, 2486–2499.

[7] V. G. Panferov, I. V. Safenkova, A. V. Zherdev, B. B. Dzantiev, *Appl. Biochem. Microbiol.* **2021**, *57*, 143–151.

[8] L. Roy, P. Buragohain, V. Borse, *Biosens. Bioelectron. X* **2022**, *10*, 100098.

[9] J. Li, M. A. Baird, M. A. Davis, W. Tai, L. S. Zweifel, K. M. A. Waldorf, M. Gale, L. Rajagopal, R. H. Pierce, X. Gao, *Nat. Biomed. Eng.* **2017**, *1*, DOI 10.1038/s41551-017-0082.

[10] N. A. Taranova, A. E. Urusov, E. G. Sadykhov, A. V. Zherdev, B. B. Dzantiev, *Microchim. Acta* **2017**, *184*, 4189–4195.

[11] N. A. Taranova, V. D. Slobodenuyk, A. V. Zherdev, B. B. Dzantiev, *RSC Adv.* **2021**, *11*, 16445–16452.

[12] Y. Shen, G. Shen, *ACS Omega* **2019**, *4*, 5083–5087.

[13] X. Huang, Y. Zhou, L. Ding, G. Yu, Y. Leng, W. Lai, Y. Xiong, X. Chen, *Small* **2019**, *15*, 1903861.

[14] A. S. Avaro, Y. Sun, K. Jiang, S. S. Bahga, J. G. Santiago, *Anal. Chem.* **2021**, *93*, 15768–15774.

[15] B. Ma, Y.-Z. Song, J.-C. Niu, Z.-Y. Wu, *Lab Chip* **2016**, *16*, 3460–3465.

[16] World Health Organization, Performance Evaluation Acceptance Criteria for HBsAg In vitro diagnostics in the context of WHO Prequalification

[17] U.S. Department of Health and Human Services Food and Drug Administration, Adequate and Appropriate Donor Screening Tests for Hepatitis B; Hepatitis B Surface Antigen (HBsAg) Assays Used to Test Donors of Whole Blood and Blood Components, Including Source Plasma and Source Leukocytes **2007**.

[18] T. Rosenfeld, M. Bercovici, *Lab Chip* **2018**, *18*, 861–868.

[19] M. Bercovici, C. M. Han, J. C. Liao, J. G. Santiago, *Proc. Natl. Acad. Sci. U. S. A.* **2012**, *109*, 11127–11132.

[20] M. Bercovici, G. V. Kaigala, K. E. MacH, C. M. Han, J. C. Liao, J. G. Santiago, *Anal. Chem.* **2011**, *83*, 4110–4117.

[21] F. Paratore, T. Zeidman Kalman, T. Rosenfeld, G. V. Kaigala, M. Bercovici, *Anal. Chem.* **2017**, *89*, 7373–7381.

[22] C. Eid, J. W. Palko, E. Katilius, J. G. Santiago, *Anal. Chem.* **2015**, *87*, 6736–6743.

[23] P. Nanthasurasak, J. M. Cabot, H. H. See, R. M. Guijt, M. C. Breadmore, *Anal. Chim. Acta* **2017**, *985*, 7–23.

[24] B. Y. Moghadam, K. T. Connelly, J. D. Posner, *Anal. Chem.* **2015**, *87*, 1009–1017.

[25] B. Y. Moghadam, K. T. Connelly, J. D. Posner, *Anal. Chem.* **2014**, *86*, 5829–5837.

[26] A. T. Bender, M. D. Borysiak, A. M. Levenson, L. Lillis, D. S. Boyle, J. D. Posner, *Anal. Chem.* **2018**, *90*, 7221–7229.

[27] B. P. Sullivan, A. T. Bender, D. N. Ngyuen, J. Y. Zhang, J. D. Posner, *J. Chromatogr. B Anal. Technol. Biomed. Life Sci.* **2021**, *1163*, 122494.

[28] A. T. Bender, B. P. Sullivan, J. Y. Zhang, D. C. Juergens, L. Lillis, D. S. Boyle, J. D. Posner, *Analyst* **2021**, *146*, 2851–2861.

[29] A. Sena-Torralba, R. Alvarez-Diduk, C. Parolo, H. Torné-Morató, A. Müller, A. Merkoçi, *Anal. Chem.* **2021**, *93*, 3112–3121.

[30] C. Eid, J. G. Santiago, *Lab Chip* **2018**, *18*, 11–26.

[31] C. Kim, Y. K. Yoo, S. Il Han, J. Lee, D. Lee, K. Lee, K. S. Hwang, K. H. Lee, S. Chung, J. H. Lee, *Lab Chip* **2017**, *17*, 2451–2458.

[32] T. Zeidman Kalman, R. Khalandovsky, E. Tenenbaum Gonikman, M. Bercovici, *Angew. Chemie Int. Ed.* **2018**, *57*, 3343–3348.

[33] Y. Liu, C. Le, D. L. Tyrrell, X. C. Le, X.-F. Li, *Anal. Chem.* **2020**, *92*, 6495–6501.

[34] S. C. Razo, V. G. Panferov, I. V. Safenkova, Y. A. Varitsev, A. V. Zherdev, B. B. Dzantiev, *Anal. Chim. Acta* **2018**, *1007*, 50–60.

[35] J. Yang, K. Wang, H. Xu, W. Yan, Q. Jin, D. Cui, *Talanta* **2019**, *202*, 96–110.

[36] K. V. Serebrennikova, A. N. Berlina, D. V. Sotnikov, B. B. Dzantiev, A. V. Zherdev, *Biosensors* **2021**, *11*, 512.

[37] Z. Qin, W. C. W. Chan, D. R. Boulware, T. Akkin, E. K. Butler, J. C. Bischof, *Angew. Chemie - Int. Ed.* **2012**, *51*, 4358–4361.

[38] E. Climent, K. Rurack, *Angew. Chemie Int. Ed.* **2021**, *60*, 26287–26297.

Graphical abstract

Conventional assay

Electrophoresis-assisted multilayer assembly
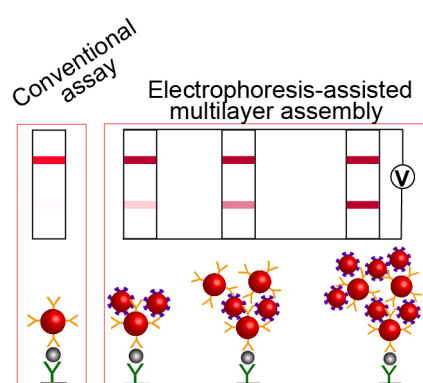
We report a universal approach for reducing the limit of detection of lateral flow immunoassay. This approach utilizes electrophoresis-driven migration of biotin- and streptavidin-modified gold nanoparticles for layer-by-layer assembly of aggregates directly on the test strip. As a result, a 60-times lower limit of detection of hepatitis B antigen is achieved.

Institute and/or researcher Twitter usernames: @skrylov22345

Supplementary Information

Electrophoresis-assisted multilayer assembly of nanoparticles for sensitive lateral flow immunoassay

Vasily G. Panferov,[a,b,c] Nikita A. Ivanov,[a,b] Tony Mazzulli,[d] Davor Brinc,[e] Vathany Kulasingam,[e] and Sergey N. Krylov*[a,b]

[a]   Dr. V. G. Panferov, N. A. Ivanov, Prof. S. N. Krylov
        Department of Chemistry, York University, 4700 Keele Street, Toronto, Ontario M3J 1P3, Canada
        E-mails: vpanf@yorku.ca, nivanov@yorku.ca, skrylov@yorku.ca
[b]   Dr. V. G. Panferov, N. A. Ivanov, Prof. S. N. Krylov
        Centre for Research on Biomolecular Interactions, York University, 4700 Keele Street, Toronto, Ontario M3J 1P3, Canada
[c]   Dr. V. G. Panferov
        A.N. Bach Institute of Biochemistry, Federal Research Centre "Fundamentals of Biotechnology" Russian Academy of Sciences, 33 Leninsky Prospect, Moscow 119071, Russia
[d]   Dr. Tony Mazzulli, Sinai Health, Toronto, 600 University Avenue, Toronto, Ontario M5G 1X5, Canada
        E-mail: tony.mazzulli@sinaihealth.ca
[e]   Dr. Davor Brinc, Dr. Vathany Kulasingam
        Toronto General Hospital: University Health Network, 200 Elizabeth St., Toronto, Ontario M5G 2C4, Canada
        E-mails: davor.brinc@uhn.ca, dr.vathany.kulasingam@uhn.ca

Abstract: Lateral flow immunoassay (LFIA) is a rapid, simple, and inexpensive method for point-of-need analysis. A major limitation of LFIA is a high limit of detection (LOD), which impacts its diagnostic sensitivity. To overcome this limitation, we introduce a signal-enhancement procedure that is performed after completing LFIA and involves controllably moving biotin- and streptavidin-functionalized gold nanoparticles along the test strip by electrophoresis. The nanoparticles link to immunocomplexes and each other forming multilayer aggregates on the test strip, thus, enhancing the signal. Here, we demonstrate lowering the LOD of hepatitis B surface antigen from approximately 8 to 0.12 ng/mL, making it clinically acceptable. Testing 76 clinical samples of serum and plasma for hepatitis B revealed that signal enhancement increased diagnostic sensitivity of LFIA from 72% to 98% while not affecting its 90% specificity. Electrophoresis-driven detection enhancement of LFIA is universal (antigen-independent), takes two minutes, and can be performed by an untrained person using an inexpensive accessory.

Table of Contents

Experimental Procedures

Materials

Monoclonal antibodies to HBsAg (clones No 4, 5, 6; catalog numbers ABHBS-0404, ABHBS-0405, ABHBS-0406, respectively), recombinant HBsAg (catalog number AGHBS-0120), and goat-anti-mouse anti-species antibodies (catalog number ABGAM-0500) were purchased from Arista Biologicals (Allentown, PA, USA). Human serum, salts, acids, and solvents were purchased from Sigma Aldrich (Oakville, ON, Canada). Nitrocellulose membranes (Millipore 75), cellulose absorbent pads (Millipore C083), and glass-fiber membranes (Millipore G041) were purchased from Millipore (Billerica, MA, USA). Serum and plasma samples were provided by Sinai Health and Toronto General Hospital.

Synthesis and conjugation of gold nanoparticles

Gold nanoparticles (GNP) were synthesized by the reduction of $HAuCl_4$ with sodium citrate.[1] All glassware were washed with aqua regia. MilliQ water (96 mL) was mixed with 1% $HAuCl_4$ (1 mL) and heated to the boiling point during continuous mixing. After boiling started, 1% sodium citrate (3 mL) was injected, and the mixture was boiled for 30 min. An Allihn condenser was used to avoid water evaporation during synthesis. Synthesized nanoparticles were stored at +4°C.

For conjugation with GNP, biotinylated antibodies were synthesized. For the biotinylation, antibodies (6 µM) in 20 mM 4-(2-hydroxyethyl)-1-piperazineethanesulfonic acid (HEPES) buffer pH 7.5 were mixed with 15-molar excess of biotinamidohexanoyl-6-aminohexanoic acid N-hydroxysuccinimide ester and incubated for two hours at room temperature. After the incubation, biotinylated antibodies were purified from the excess of activated biotin ester using Amicon centrifugal filters with cut-off 100 kDa provided by Sigma Aldrich (Oakville, ON, Canada). Biotinylated antibodies were stored at 4°C in 10 mM tris(hydroxymethyl)aminomethane (Tris) buffer containing 0.02% sodium azide, pH 8.

Physical adsorption of proteins was used for the conjugation with GNP. For conjugation with streptavidin (GNP-Str), the pH of GNP was adjusted to 6.5 using 0.5 M K_2CO_3, and streptavidin was added to the final concentration of 10 µg/mL The mixture was incubated for 2 h, and particles were concentrated by centrifugation 16,000×g for 15 min at 4°C. The conjugates were redispersed in MilliQ water containing 0.02% sodium azide and were stored at 4°C. For conjugation with biotinylated antibodies (GNP-Ab$_B$), the pH of GNP was adjusted to 9.0 using 0.5 M K_2CO_3, and antibodies were added to the final concentration of 12 µg/mL. Incubation and centrifugation of conjugates were similar to the above-described streptavidin conjugates.

Assembly of test strips

A custom reagent dispenser consisting of a syringe pump "Pump 11 Elite" from Harvard Instruments (Holliston, MA, USA) and a 3D moving platform from Sain Smart Genmitsu CNC router machine was used. Monoclonal antibodies (clone 6) were dispensed as the test line, anti-species antibodies were dispensed as the control line. The antibodies were diluted by 20 mM sodium phosphate buffer, pH 7.5 to the final concentration of 1 mg/ml and dispensed at a rate of 1.5 µL/cm. Conjugate of GNP with biotinylated antibodies (clone 4) was diluted with conjugate buffer (20 mM Tris-acetate, pH 7.6, 1% bovine serum albumin, 0.5% lactose, 0.05% sodium azide, 0.03% sodium dodecyl sulfate) to $OD_{520\,nm}$ = 0.6 measured in a cuvette with a 1-mm optical pathlength. The fiberglass membrane (width 4 mm) was soaked with the diluted conjugate (2.5 µL per mm of length) and dried at room temperature for 12 h. Cellulose and fiberglass membranes were glued to a nitrocellulose membrane. The membranes were cut manually to the test strips with a width of 4 mm and stored at room temperature in zip pockets.

Manufacturing of test strip holder

Holders of test strips for electrophoresis were designed in Solid Edge (Siemens Digital Industries Software) and fabricated of poly(methyl methacrylate) plastic according to our previously developed fabrication procedure.[2] The holders were fabricated using MODELA MDX-540 Benchtop Milling Machine from Roland DGA (Irvine, CA, USA). Platinum wires electrodes (0.25 mm) were inserted into the buffer reservoirs on both sides. Solid Edge files of the holders' geometry are available as supporting materials.

Assay performance

Conventional and enhanced LFIA were performed in buffer, human serum, human plasma, and capillary blood. Human serum was spiked with HBsAg. Spiked serum was diluted by 50 mM sodium borate buffer, pH 8.1, containing 0.06% 2-hydroxyethyl cellulose (HEC, MW 380 kDa), 0.08% sodium dodecyl sulfate. Capillary blood was collected from a healthy volunteer using a lancet pen device. Ethylenediaminetetraacetic acid (final concentration 2 mg/mL) was added to avoid coagulation. Capillary blood was diluted 50 times with the running buffer and used for LFIA.

For the conventional LFIA, test strips were vertically immersed in the sample (100 µL) and incubated for 5 min. After 5 min incubation, the test strips were scanned using Epson V600 scanner, and digital images of the test strips were used for the quantification of test zone color intensity using TotalLab TL120 from Nonlinear Dynamics (Newcastle, UK). Digital images were converted to a grayscale mode and analyzed using 1D gel analysis mode of the software. The rectangular regions near the test zone were selected, background outside the test zone was substituted for each test strip. The colorimetric signal was calculated as the ratio of the zone's volume to area values. The calibration plots were obtained as the function of the measured colorimetric signals (relative units, RU) versus HBsAg concentrations (ng/mL) using OriginPro 2021 from OriginLab corporation (Northampton, MA, USA). The LOD of the assay was determined as the HBsAg concentration corresponding to the value of the colorimetric signal of the test zone higher than a value of blank samples (n = 3, Ablank) plus three standard deviations of Ablank (SDblank), i.e., LOD = A_{blank} + 3 SD_{blank}.

After performing the conventional LFIA, the test strips were used in the enhanced LFIA. The ends of the test strips were immersed into two wells containing running buffer (the same as used for the conventional LFIA) and Pt-wire electrodes. The voltage was applied (current was limited to 1 mA) using electrophoresis power supply EPS 3501 from Amersham Pharmacia Biotech (Amersham, UK). Each of the GNP-Str and GNP-Ab$_B$ conjugates was diluted with the running buffer to $OD_{520\,nm}$ = 0.4 measured in a cuvette with a 1-mm

optical pathlength. First, GNP-Str was introduced (1.5 μL), followed by the same volume of GNP-Ab$_B$. The colorimetric signals of TZs and LOD were evaluated as described above for the conventional LFIA.

Clinical validation

Serum and plasma samples were analyzed by testing laboratories in Sinai Health and Toronto General Hospital using Abbott chemiluminescent microparticle immunoassay Alinity i for the hepatitis B antigen by Abbott Laboratories (HBsAg 08P08 quantitative assay, reactive: > 0.05 IU/mL, Alinity I, Abbott Diagnostics, Abbott Park, IL, USA). In summary, 54 positive samples (HBsAg in a range of 0.05 to 124,925 IU/mL) and 22 negative samples (HBsAg below 0.05 IU/mL) were used for LFIA validation. Each sample was tested at least in two replicates. The performance of conventional and enhanced LFIA is described in section assay performance.

Measuring the temperature of the test strip

The temperature of test strips during electrophoresis was measured using the high-resolution thermal imaging infrared camera Fluke TiX580 (Everett, WA, USA). The electrophoresis was performed as described in section assay performance. The recorded temperature profiles were analyzed using SmartView Classic ver. 4.4. from Fluke Thermography (Everett, WA, USA). The kinetics of temperature on test strips were recorded for 10 values of voltage applied: 0, 40, 60, 80, 100, 150, 200, 250, 300, and 350 V. After two min of electrophoresis, the recorded temperature was plotted against voltage using OriginPro 2021.

Results and Discussion

Characterization of nanoparticles
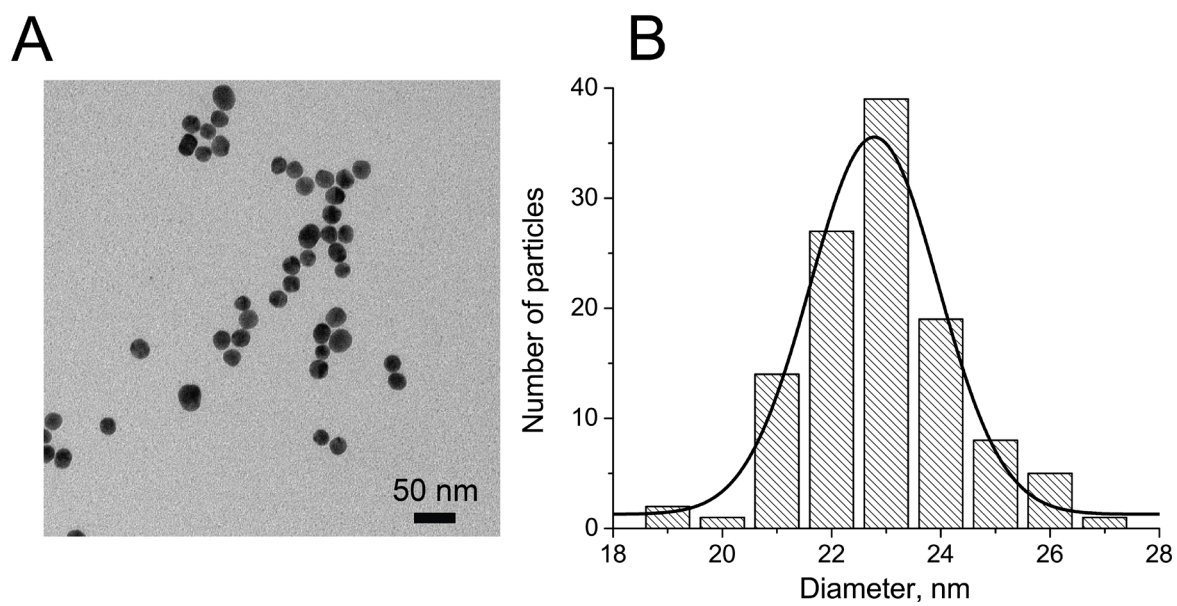
Figure S1. Characterization of GNP. **A**: microphotograph of GNP. **B**: histogram of size distribution for GNP, mean diameter 22.7 ± 1.9 nm.
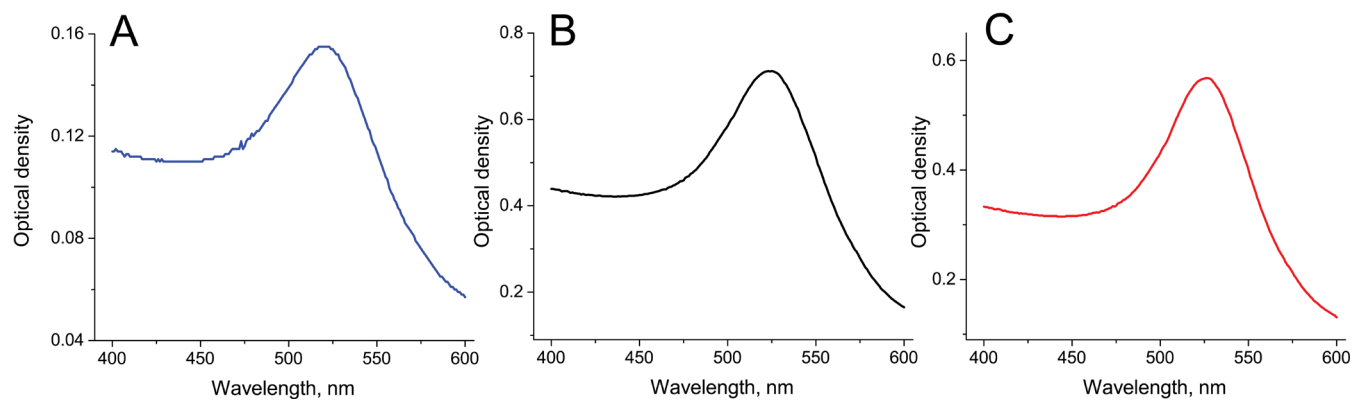
Figure S2. Optical spectra of nanoparticles. **A**: GNP. **B**: GNP-Ab_B conjugate. **C**: GNP-Str conjugate.

Affine binding of conjugates
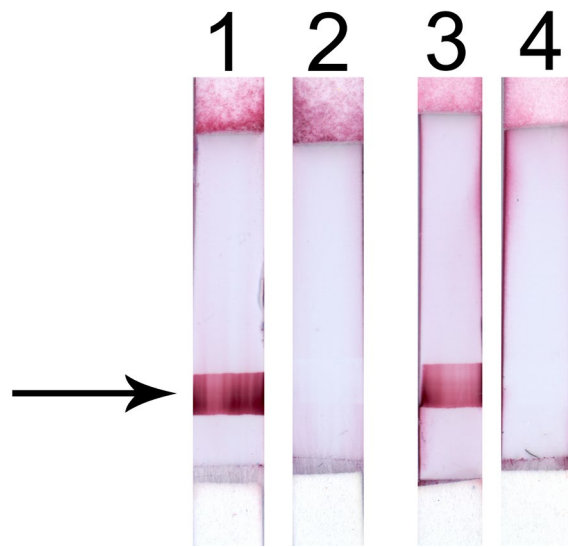
Figure S3. Affine capturing of GNP conjugates. Binding zones shown with the arrow contain Ab_B (test strips 1 and 2) and Str (test strips 3 and 4). GNP-Str conjugate was applied to test strips 1 and 4. GNP-Ab_B conjugate was applied to test strips 2 and 3.

Optimization of LFIA
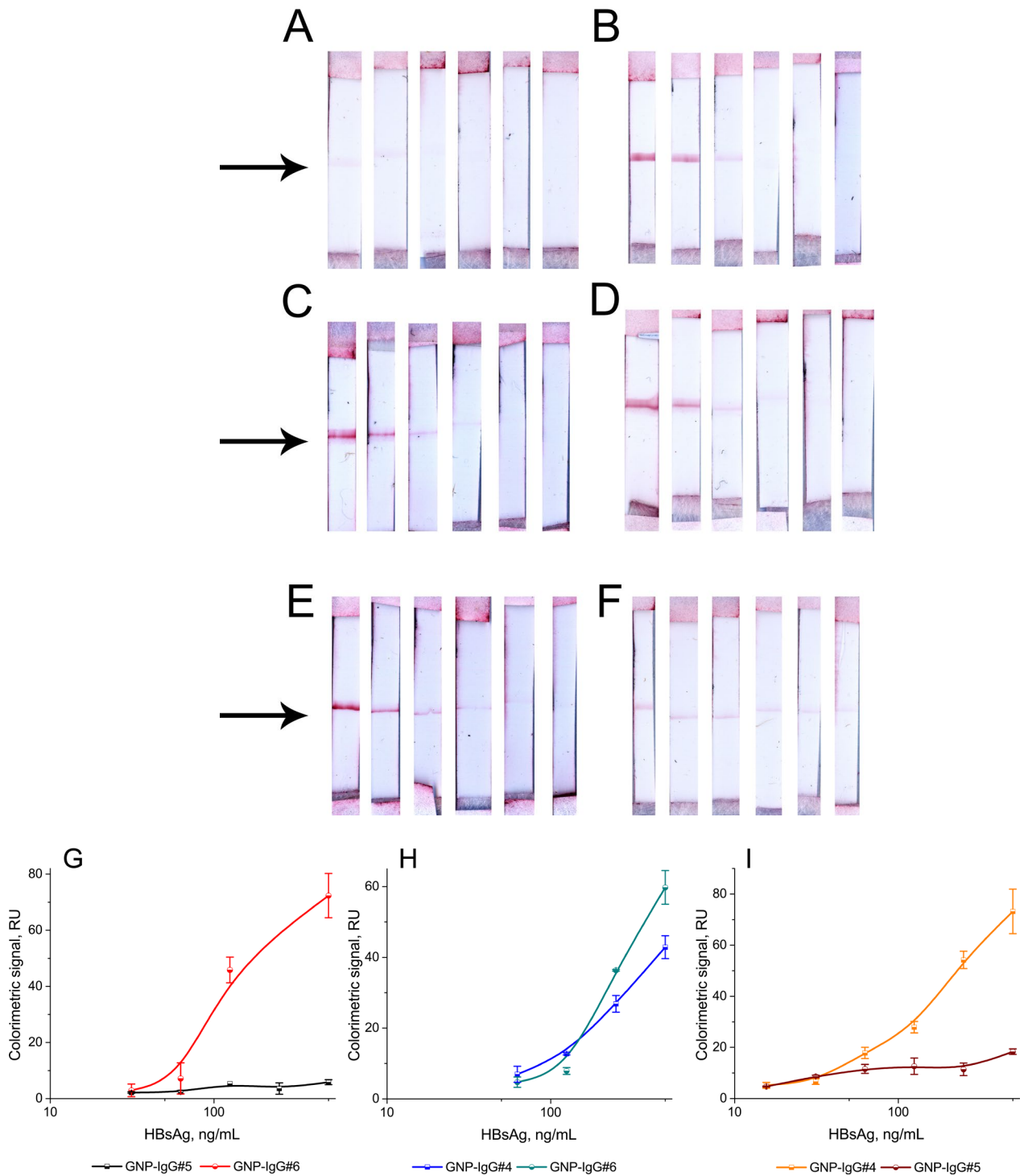
Figure S4. Performance of LFIA with various combinations of three monoclonal antibodies. **A**: clone 4 on the membrane, clone 5 on GNP. **B**: clone 4 on the membrane, clone 6 on GNP. **C**: clone 5 on the membrane, clone 4 on GNP. **D**: clone 5 on the membrane, clone 6 on GNP. **E**: clone 6 on the membrane, clone 4 on GNP. **F**: clone 6 on the membrane, clone 5 on GNP. Concentrations of HBsAg (from left to right) are 500, 250, 125, 62.5, 31.3, and 15.6 ng/mL. **G**: calibration plots for test strips shown in panels A and B. **H**: calibration plots for test strips shown in panels C and D. **I**: calibration plots for test strips shown in panels E and F.

Optimization of the running buffer for electrophoresis

Table S1. Compositions of the running buffer.

Buffer composition	Additives to the buffer	GNP-Str electrophoretic migration
50 mM Tris-acetate, pH 8.2.	-	Figure S5A
	0.1% 2-hydroxyethyl cellulose, MW 380 kDa (HEC)	Figure S5B
	0.2% HEC	Figure S5C
	0.2% HEC, 0.04% SDS, 0.025% Triton X-100	Figure S5D
	0.2% HEC, 0.08% SDS, 0.025% Triton X-100	Figure S5E
	0.3% HEC	Figure S5F
	0.5% HEC	FigureS5G
	0.7% HEC	Figure S5H
	0.1% HEC, 0.05% Tween-20	Figure S5I
	0.1% HEC, 0.01% Triton X-100	FigureS5J
	0.08 % HEC, 0.05% Triton X-100	FigureS5K
	0.08% HEC, 0.025% Triton X-100, 0.08% SDS	FigureS5L
	0.08 % HEC, 0.025 % Triton X-100, 0.04 % SDS	FigureS5M
	0.08 % HEC, 0.05% Triton X-100, 0.04 % SDS	Figure S5N
	0.05% Triton X-100, 0.04 % SDS	FigureS5O
50 mM Tris-borate buffer, pH 8.3	0.1 %HEC	FigureS5P
	0.1% HEC, 0.025 % Triton X-100	FigureS5Q
50 mM sodium phosphate buffer, pH 7.4	0.1 % Triton X-100	FigureS5R
	0.1 %HEC	FigureS5S
	0.1% HEC, 0.05% Triton X-100, 0.5% BSA	FigureS5T
	0.1%HEC, 0.05% Triton X-100	Figure S5U
	0.1%HEC, 0.05% Triton X-100	Figure S5V
	0.1% HEC, 0.05% Triton X-100, 0.08% SDS	Figure S5W
	0.1% HEC, 0.025% Triton X-100, 0.08% SDS	Figure S5X
	0.1% HEC	Figure S5Y
	0.1% HEC, 0.05% Triton X-100	Figure S5Z
	0.05% Triton X-100	Figure S5AB1

50 mM HEPES, pH 7.6	0.2% HEC, 0.08% SDS	Figure S5 AB2
50 mM sodium borate buffer, pH 8.1	-	Figure S5 AB3
	0.08% HEC, 0.03% SDS	Figure S5 AB4
	0.5% BSA	Figure S5 AB5
	0.5% BSA + 0.05% Triton X-100	Figure S5 AB6
	0.05% Triton X-100	Figure S5 AB7

A

B

C

D

E

F

G

3
min
→

H

I

J

K

3 min →

5 min →

5 min →

Changing of polarity →

L
M
N
O
P
Q
R
S

13

5 min →

1 min →

5 min →

2 min →

5 min →

4 min →

4 min →
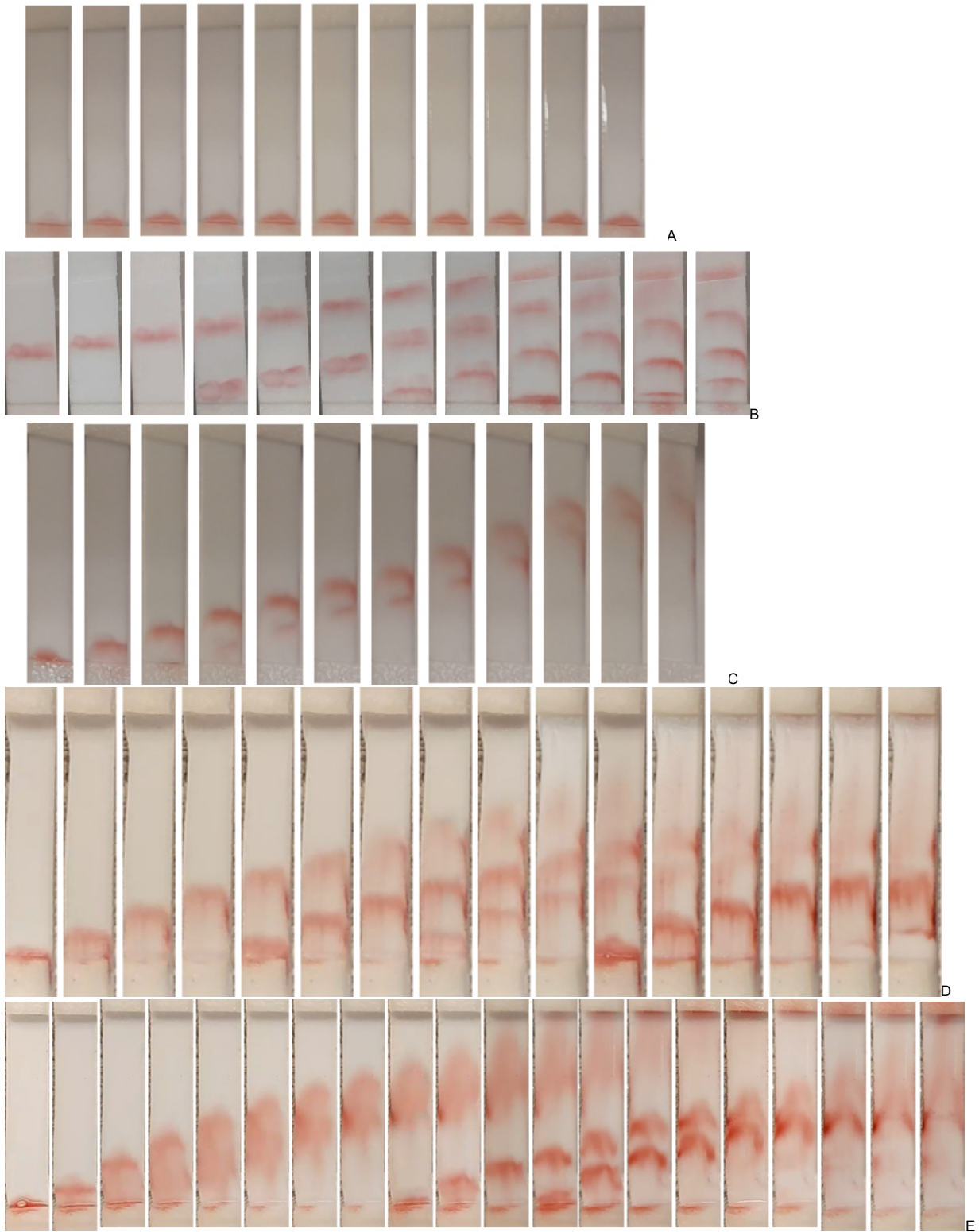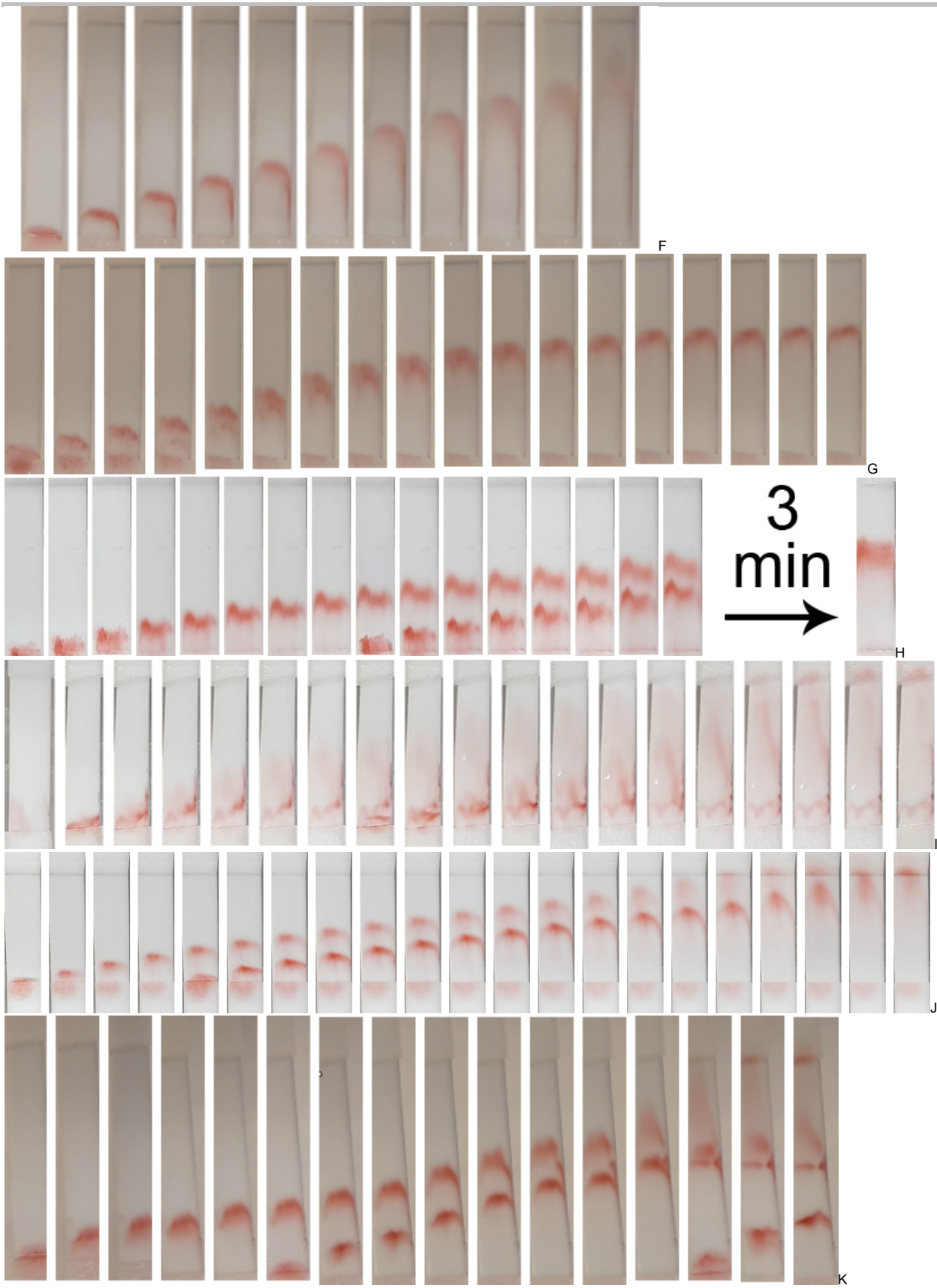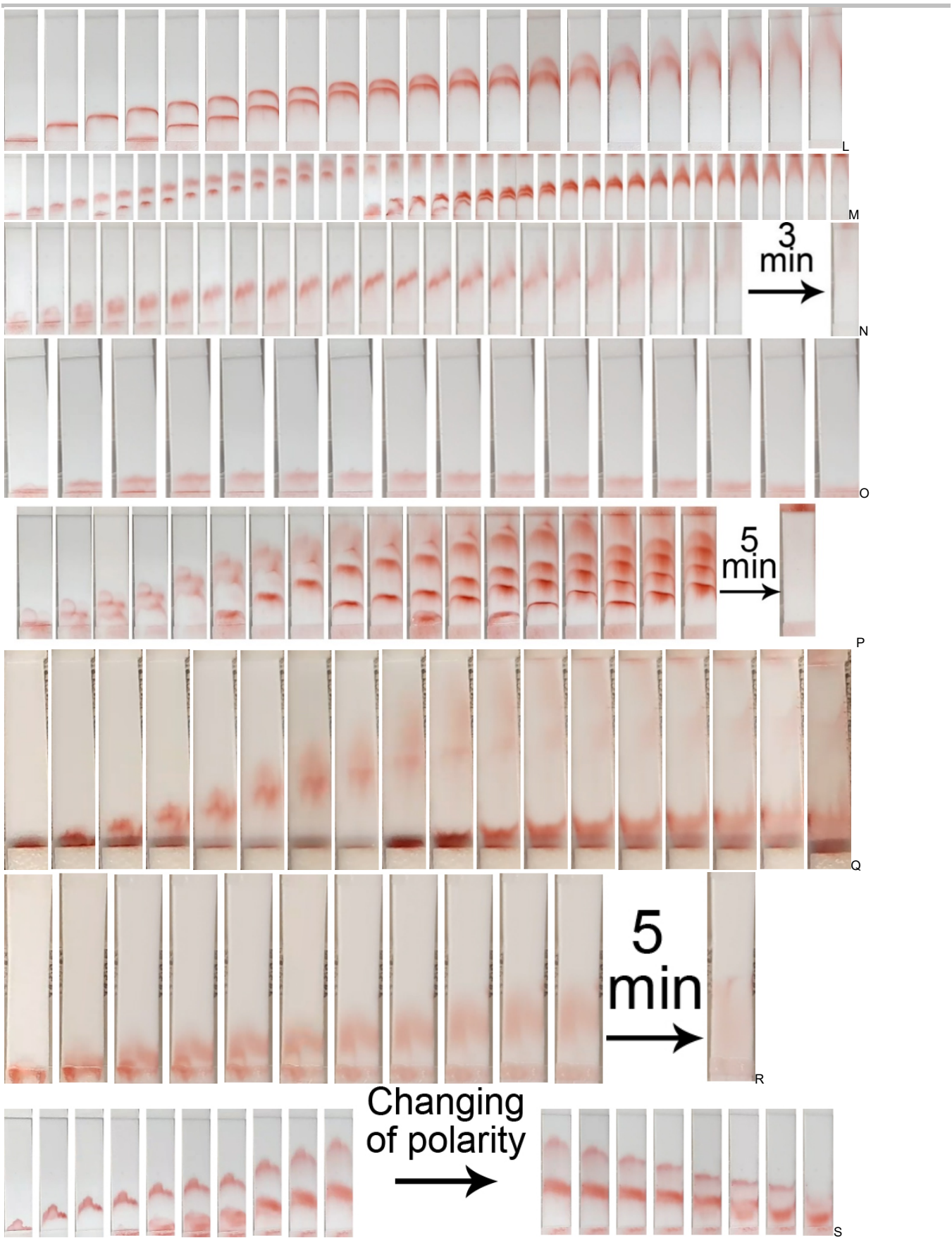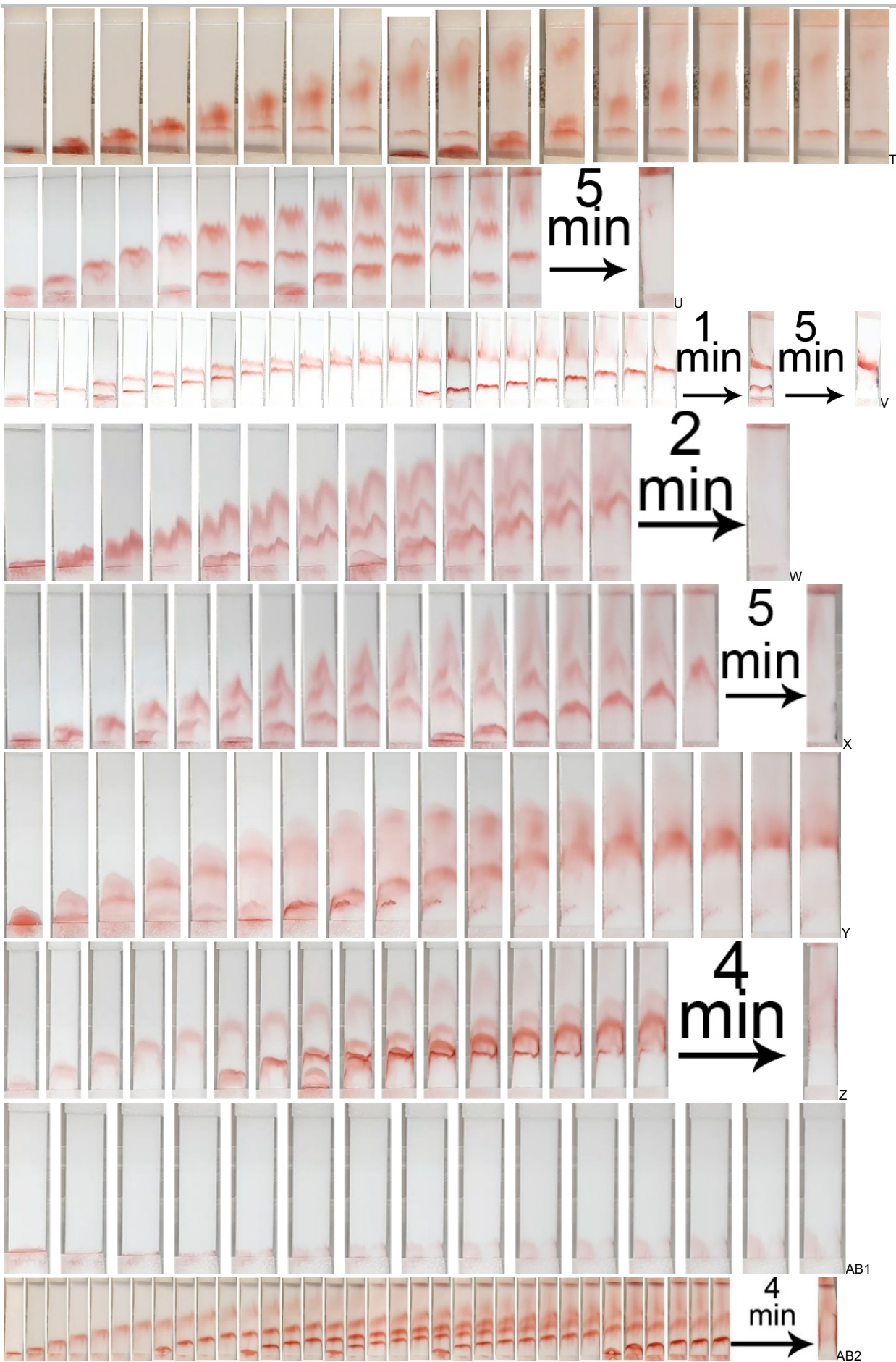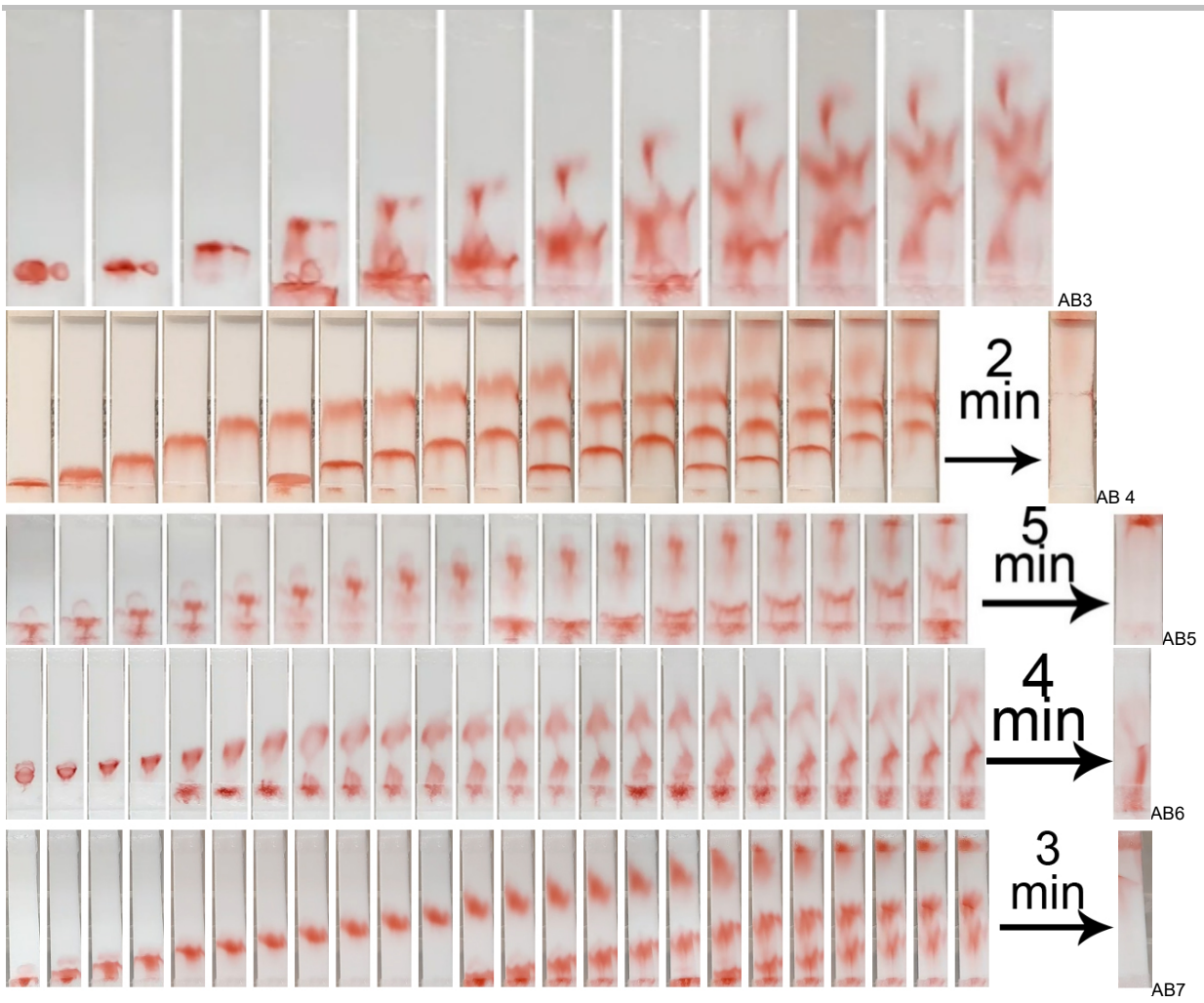
Figure S5. Progressive images (from left to right, 20-s time interval) of a test strip for various buffer compositions.

The geometry of the test strip holder
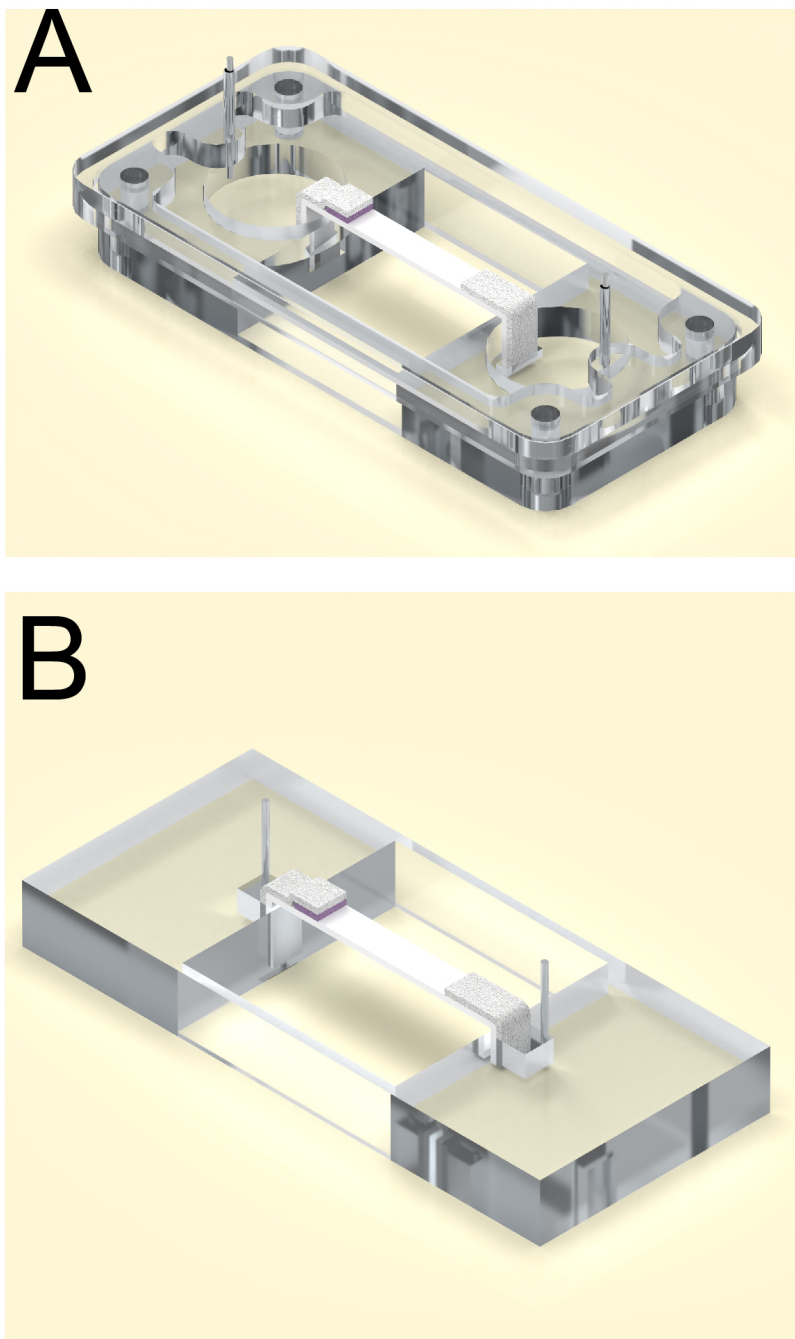
Figure S6. The geometry of the test strip holder for electrophoresis. A: the model of the holder with large-volume reservoirs. B: the model of the holder with small-volume reservoirs.

Comparison of LOD reduction approaches

Table S2. LOD reduction of LFIA achieved by the nanoparticles-crosslinking.

Target	LOD reduction	Assay performance	Reference
Prostate-specific antigen	2.5 times	Two binding conjugates (GNP-BSA_B-Ab - GNP-neutravidin) incubated on the test strip after assay performance	[3]
Procalcitonin	4 times	GNP-Ab_B crosslinked by streptavidin dried at membrane	[4]
Troponins I and T	3-10 times	Three binding conjugates (GNP-BSA_B-GNP-Str- GNP-Ab_B) dried on the membrane	[5]
Furazolidone	5 times	Two binding conjugates (GNP-Ab – GNP-antispecies Ab) dried on the single membrane	[6]
Influenza virus A protein	8 times	Two binding conjugates (GNP-Ab-BSA_B- GNP-anti-biotin- Ab) dried on two separate membranes	[7]
Streptomycin	10 times	GNP-Str crosslinked by -Ab_B and BSA_B during preincubation	[8]
Biotinylated DNA sequence	10 times	Two binding conjugates (GNP-Ab-BSA- GNP-anti-BSA-Ab) crosslinked during preincibation	[9]
Melamine	10-25 times	Two binding conjugates (GNP-Ab-BSA – GNP-anti-BSA- Ab) dried at two membranes	[10]
Carcinoembryonic antigen	20 times	Two binding magnetic nanoparticles conjugates (magnetic nanoparticle – DNA_B-magnetic nanoparticle Str) dried on two separate membranes	[11]
Procalcitonin	10-30 times	Three binding conjugates (GNP-BSA_B-GNP-Str- GNP-Ab_B) dried on the membrane	[12]
Thrombin	30 times	Two binding conjugates GNP-DNA_1-GNP-DNA_2 by hybridization between complementary DNA_1 and DNA_2 strands	[13]
Hepatitis B surface antigen	30 times	Two binding conjugates (GNP-Str- GNP-Ab_B), dried on two separate membranes	[14]
Potato virus X	32 times	Two binding conjugates (magnetic nanoparticles-Ab_B and GNP-Str) crosslinked during preincubation and concentrated by a magnet	[15]
Hepatitis B surface antigen	64.5 times	Electrophoresis-assisted post-assay binding of GNP-AbB and GNP-Str	This article

Comparison of LFIA for HBsAg

Table S3. Comparison of the LFIAs for HBsAg.

Label	Assay performance	LOD ng/mL	Reference
Magnetic nanoparticles	Calibration in buffer, 20 min,	1	[16]
Red-colored silica particles	Calibration in buffer, 10 min, dynamic range 5–500 ng/mL	0.97	[17]
Gold nanoparticles	Calibration in serum, 25 min	0.46	[18]
Ultramarine blue particles	Calibration in buffer, 15 min, dynamic range 1–50 ng/mL,	0.37 in buffer 5 in fetal calf serum	[19]
Eu (III) chelate microparticles	15 min, linear range 0.63–640 IU/mL, fluorescence reader	0.31 IU/mL	[20]
CdSe/ZnS quantum dots	Calibration in buffer, 35 min, fluorescence strip reader	0.156	[21]
Au@Pt-nanoparticle-decorated blue-silica-nanoparticle	Calibration in buffer and fetal calf serum 15 min, dynamic range 0.5–10 ng/mL,	0.13 in buffer 0.5 in serum	[22]
Horseradish peroxidase-conjugated GNP	Human serum 20 min, addition of freshly-prepared enzyme substrate through additional paper pads	0.12	[23]
Polydiacetylene vesicles	Calibration in buffer, 15 min, fluorescence reader	0.1 by fluorescence detection 1 by colorimetric detection	[24]
Magnetic nanoparticles	Calibration in human serum, 30 min, magnetic reader Dynamic range 0.08–30 ng/mL	0.08	[25]
CdSe/ZnS quantum dot beads	Calibration in fetal calf serum,15 min, fluorescence reader	0.075	[26]
Gold nanoparticles	Calibration in buffer, 10 min, dynamic range 0.1–30 ng/mL	0.06	[14]
Upconverting nanoparticle	Calibration in serum and whole blood, photoluminescence reader, 30 min	0.05 IU/mL in serum 0.2 IU/mL in whole blood	[27]
Europium chelate–loaded silica nanoparticles	Calibration in buffer, 30 min, fluorescence reader, dynamic range 0.05–3.13 ng/mL	0.03	[28]
CdS wires	Calibration in serum, linear range 0.02-100 ng/mL, fluorescence detector	0.02	[29]
Gold nanoparticles	Calibration in serum, linear range 0–62.5 ng/mL, performance within 10 min. Additional equipment: power supply	0.12	This work

Linear range of enhanced LFIA
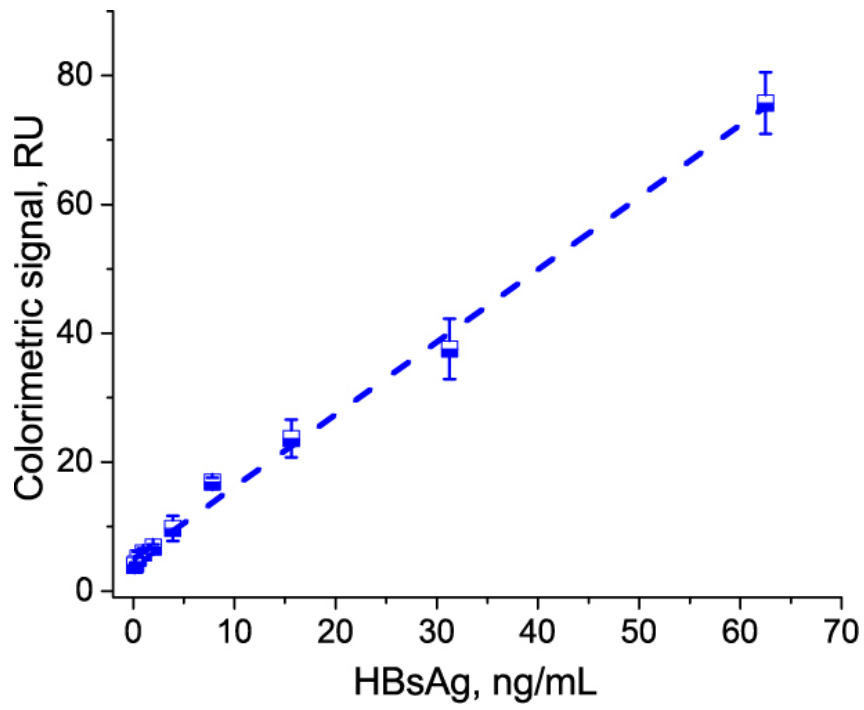
Figure S7. The dependence of test zone colorimetric signal from HBsAg concentrations. Linear regression is shown with the blue dashed line ($R^2 = 0.994$).

Correlation between spiked and measured concentration of HBsAg
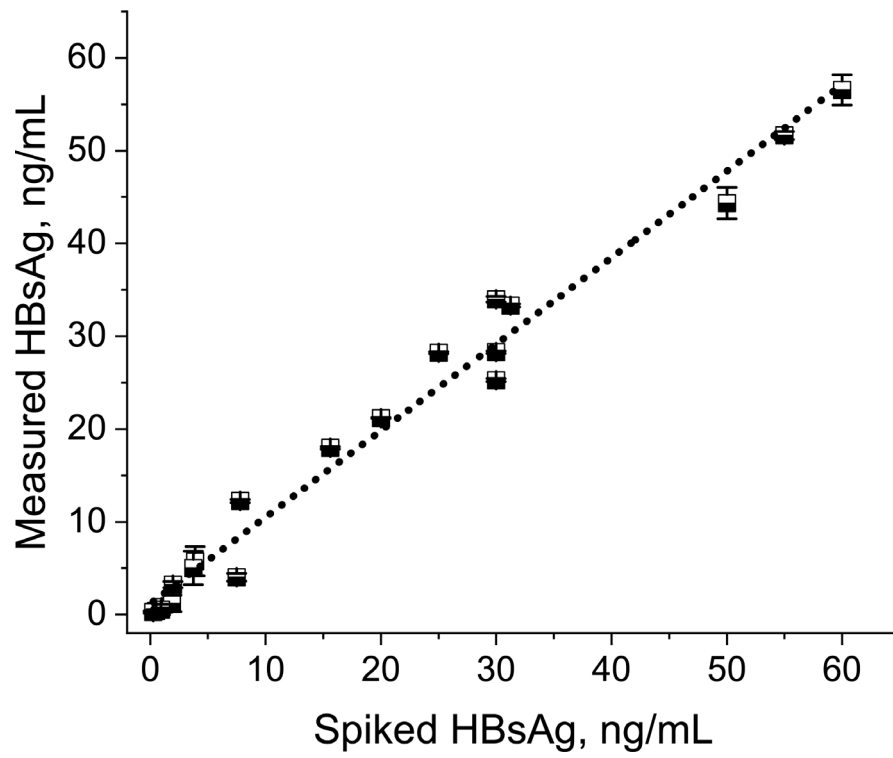
Figure S8. Correlation between spiked and measured concentration of HBsAg in human serum. Linear regression is shown with the black dotted line (R^2 = 0.979).
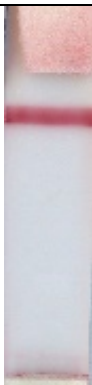
LFIA of HBsAg in clinical samples
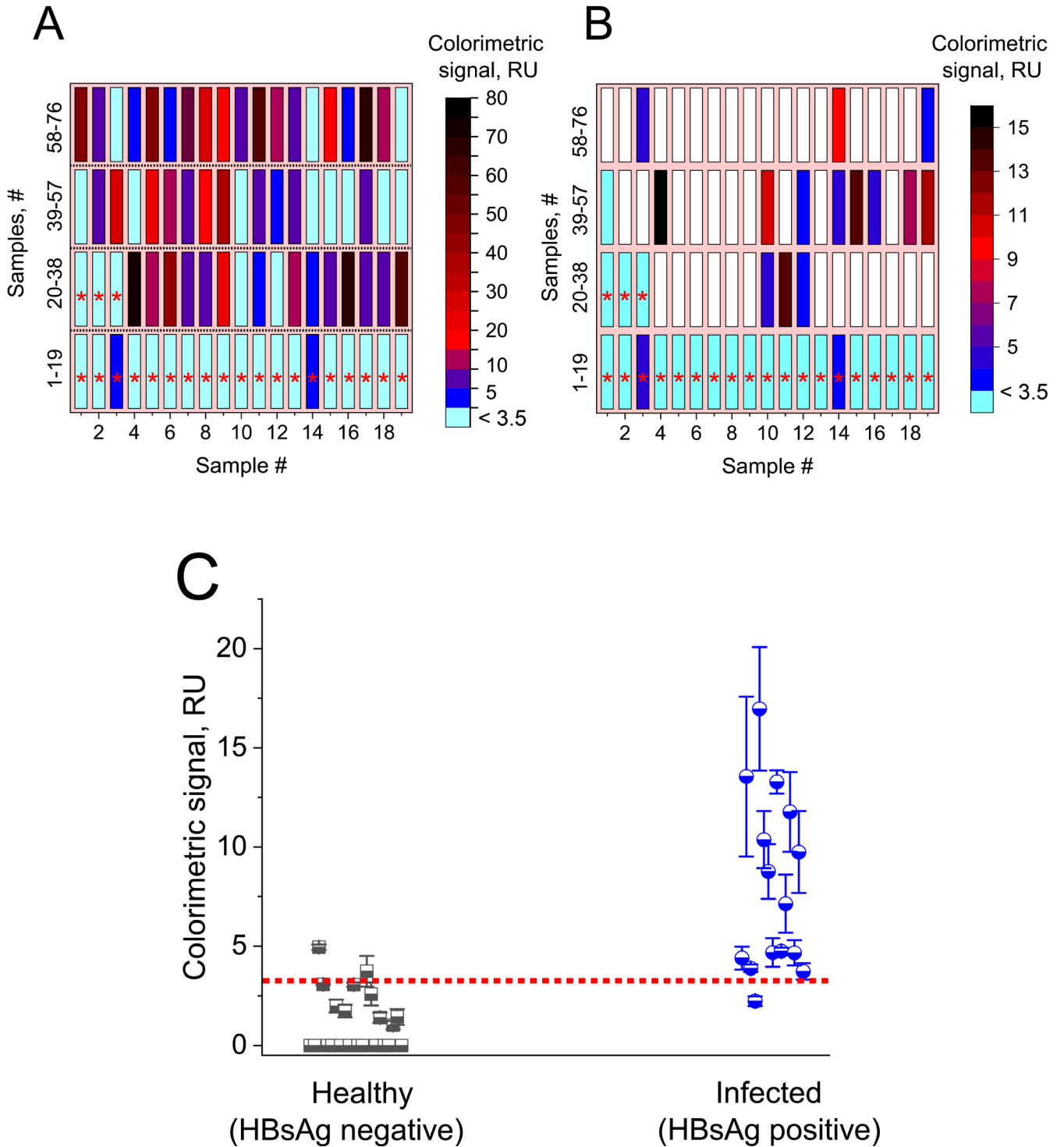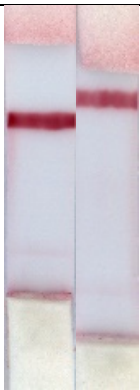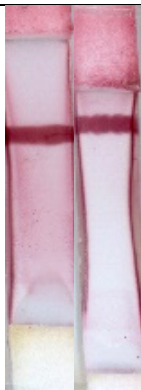
Figure S9. Results of lateral flow immunoassay of serum and plasma samples. **A**: colorimetric signals of test zones for conventional LFIA. Red asterisks indicate negative samples (samples #1–22). Enhancement was performed for all samples with the colorimetric signal below 4 RU. **B**: colorimetric signals of test zones for enhanced LFIA. For samples shown with white color, enhancement was not performed. **C**: colorimetric signals of test zones for healthy (HBsAg negative) and infected (HBsAg positive, only low positive samples are shown) serum samples after enhancement. The red dotted line corresponds to the cut-off value (3.3 RU).

Table S4. Biosamples used for the validation of LFIA

Sample No, type	Patient information	Results of LFIA before enhancement	Results of LFIA after enhancement
1, serum	20 years old (yo), Female (F)		
2, serum	34 yo, F		
3, serum	35 yo, F		
4, serum	29 yo, F		

5, serum	45 yo, F		
6, serum	20 yo, F		
7, serum	69 yo, F		
8, serum	68 yo, F		

23

9, serum	69 yo, male (M)	24	
10, serum	64 yo, M		
11, serum	27 yo, M		
12, serum	76 yo, F		

13, serum	46 yo, F	25	
14, serum	77 yo, M		
15, serum	70 yo, F		
16, serum	51 yo, F		

17, serum	60 yo, M		26	
18, serum	73 yo, F			
19, serum	77 yo, M			
20, serum	46 yo, F			

21, serum	70 yo. F	27	
22, serum	70yo, F		
23, serum	30 yo, F		
24, serum	56 yo, M		

25, serum	41 yo, F	28	
26, serum	51 yo, M		
27, serum	N/A, F		
28, serum	44 yo, M		

29, plasma	60 yo, F	29	
30, plasma	49 yo, F		
31, plasma	57 yo, F		
32, plasma	46 yo, F		

33, plasma	47 yo, M		
34, plasma	49 yo, F		
35, plasma	50 yo, F		
36, plasma	51 yo, M		

37, plasma	58 yo, M		
38, plasma	40 yo, M		
39, plasma	34 yo, M		
40, plasma	55 yo, M		

41, plasma	39 yo, F		
42, plasma	59 yo, M		
43, plasma	44 yo, F		
44, plasma	38 yo, M		

32

45, plasma	45 yo, M		
46, plasma	60 yo, F		
47, plasma	38 yo, F		
48, serum	37 yo, M		

49, serum	67 yo, F	34	
50, serum	62 yo, F		
51, serum	75 yo, F		
52, serum	77 yo, F		

53, serum	75 yo, M		35	
54, serum	53 yo, M			
55, serum	61 yo, M			
56, serum	37 yo, M			

57, serum	72 yo, M		36
58, serum	44 yo, M		
59, serum	63 yo, F		
60, serum	72 yo, M		

61, serum	81 yo, F	37	
62, serum	59 yo, F		
63, serum	79 yo, M		
64, serum	50 yo, F		

65, serum,	45 yo, F		
66, serum	49 yo, M		
67, serum	38 yo, M		
68, serum	50 yo, F		

69, serum	79 yo, M		
70, serum	91 yo, M		
71, serum	66 yo, M		
72, serum	82 yo, M		

73, serum	66 yo, M	40	
74, serum	22 yo, F		
75, serum	63 yo, M		
76, serum	73 yo, F		
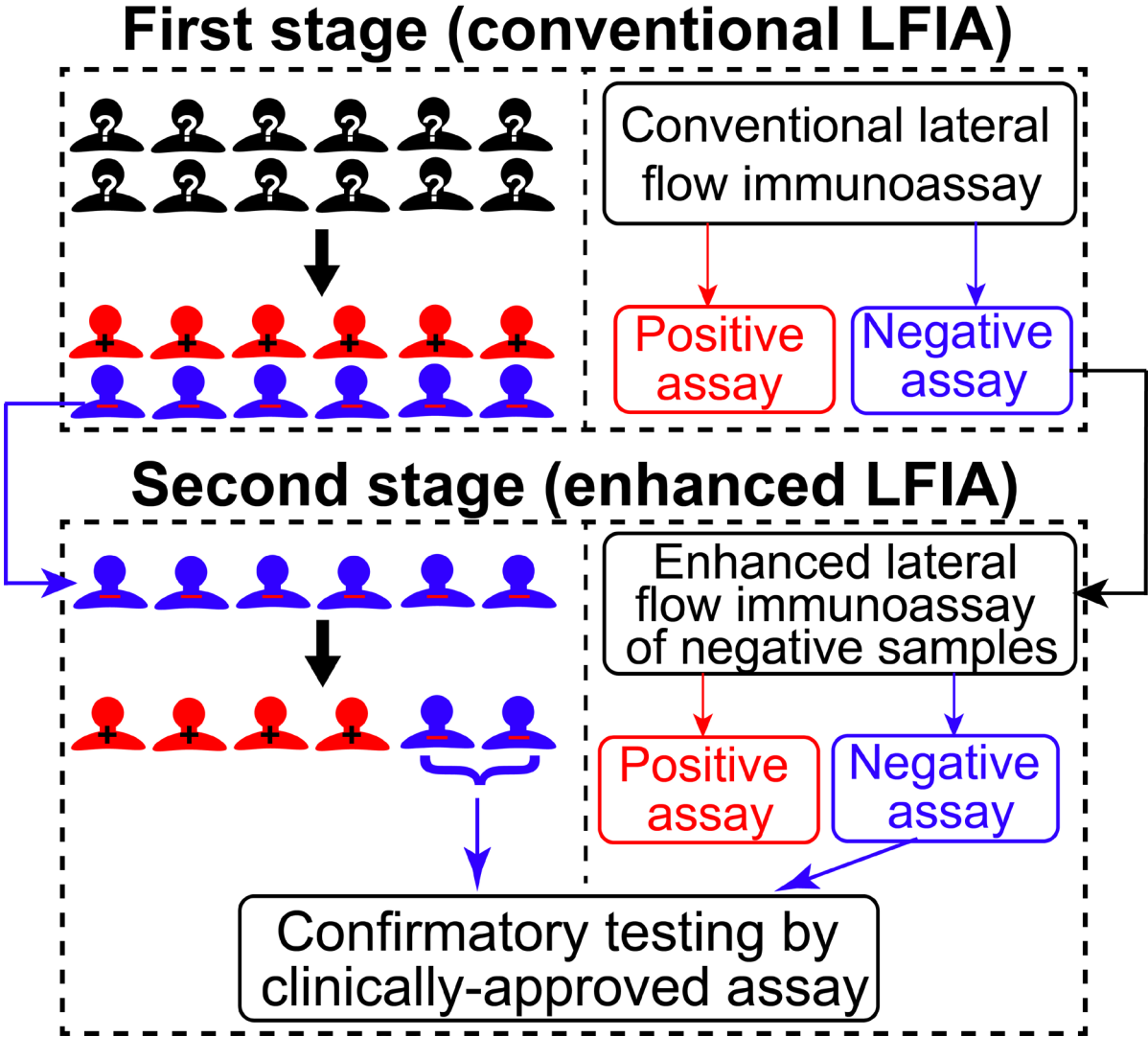
Figure S10. Two-stage performance of LFIA. **First stage**: testing of large populations using conventional LFIA. If the result is positive, the patient is diagnosed with hepatitis B. **Second stage**: all negative/low positive samples from the first stage are used in the enhancement procedure. If the result is positive, the patient is diagnosed with hepatitis B. All negative assays are further tested by clinically-approved assays to confirm the absence of hepatitis B infection.

Figure S11. Performance of LFIA in capillary blood. **A**: test strips after conventional LFIA. **B**: test strips after enhanced LFIA. The numbers above the test strips show sample numbers. **C**: colorimetric signal of test zones for test strips before and after enhancement. **D**: pixel intensity profiles along the test strips before and after enhancement.

Cost of materials for enhanced LFIA

Table S5. The estimated costs of enhanced LFIA

	Part	Material	Amount per unit	Cost in US$
Non-disposable chip (applicable for more than 1000 assays)	Body	PMMA	36 cm^3 or 2.2 in^3	$0.42 McMaster-Carr
	Electrodes	Platinum wire	2-cm long wire with 0.25 mm diameter	$6.9 Sigma Aldrich

References

[1] G. Frens, *Nat. Phys. Sci.* **1973**, *241*, 20–22.
[2] F. J. Agostino, C. J. Evenhuis, S. N. Krylov, *J. Sep. Sci.* **2011**, *34*, 556–564.
[3] M. O. Rodríguez, L. B. Covián, A. C. García, M. C. Blanco-López, *Talanta* **2016**, *148*, 272–278.
[4] K. V. Serebrennikova, J. V. Samsonova, A. P. Osipov, *Moscow Univ. Chem. Bull.* **2018**, *73*, 131–134.
[5] N. A. Taranova, V. D. Slobodenuyk, A. V. Zherdev, B. B. Dzantiev, *RSC Adv.* **2021**, *11*, 16445–16452.
[6] L. Dou, B. Zhao, T. Bu, W. Zhang, Q. Huang, L. Yan, L. Huang, Y. Wang, J. Wang, D. Zhang, *Anal. Bioanal. Chem.* **2018**, *410*, 3161–3170.
[7] N. Wiriyachaiporn, W. Maneeprakorn, C. Apiwat, T. Dharakul, *Microchim. Acta* **2015**, *182*, 85–93.
[8] O. D. Hendrickson, A. E. Urusov, D. A. Kuznetsova, A. V Zherdev, B. B. Dzantiev, A. N. Bach, *Int. J. Appl. Eng. Res.* **2017**, *12*, 13552–13564.
[9] D. K. Toubanaki, M. Margaroni, E. Karagouni, *Anal. Lett.* **2016**, *49*, 1040–1055.
[10] Y. Zhong, Y. Chen, L. Yao, D. Zhao, L. Zheng, G. Liu, Y. Ye, W. Chen, *Microchim. Acta* **2016**, *183*, 1989–1994.
[11] F. Liu, H. Zhang, Z. Wu, H. Dong, L. Zhou, D. Yang, Y. Ge, C. Jia, H. Liu, Q. Jin, J. Zhao, Q. Zhang, H. Mao, *Talanta* **2016**, *161*, 205–210.
[12] N. A. Taranova, A. E. Urusov, E. G. Sadykhov, A. V. Zherdev, B. B. Dzantiev, *Microchim. Acta* **2017**, *184*, 4189–4195.
[13] G. Shen, S. Zhang, X. Hu, *Clin. Biochem.* **2013**, *46*, 1734–1738.
[14] Y. Shen, G. Shen, *ACS Omega* **2019**, *4*, 5083–5087.
[15] S. C. Razo, V. G. Panferov, I. V. Safenkova, Y. A. Varitsev, A. V. Zherdev, B. B. Dzantiev, *Anal. Chim. Acta* **2018**, *1007*, 50–60.
[16] K. Oh, Y. S. Choi, H. Y. Yoon, N. Park, J. Kim, Y. K. Kim, *IEEE Trans. Magn.* **2014**, *50*, 1–4.
[17] Q. Yu, W. Dou, J. Liu, G. Zhao, S. Yang, D. Zhu, Y. Zhao, L. Li, *Anal. Methods* **2019**, *11*, 268–275.
[18] X. Chen, Y. Leng, L. Hao, H. Duan, J. Yuan, W. Zhang, X. Huang, Y. Xiong, *Theranostics* **2020**, *10*, 3737–3748.
[19] J. Liu, Q. Yu, G. Zhao, W. Dou, *Anal. Chim. Acta* **2020**, *1098*, 140–147.
[20] R. L. Liang, Q. T. Deng, Z. H. Chen, X. P. Xu, J. W. Zhou, J. Y. Liang, Z. N. Dong, T. C. Liu, Y. S. Wu, *Sci. Rep.* **2017**, *7*, 1–8.
[21] H. Duan, X. Chen, Y. Wu, Y. Leng, X. Huang, Y. Xiong, *Anal. Chim. Acta* **2021**, *1141*, 136–143.
[22] J. Liu, Q. Yu, G. Zhao, W. Dou, *Anal. Methods* **2019**, *11*, 6103–6110.
[23] J. H. Cho, E. H. Paek, I. I. H. Cho, S. H. Paek, *Anal. Chem.* **2005**, *77*, 4091–4097.
[24] J. Roh, S. Y. Lee, S. Park, D. J. Ahn, *Chem. - An Asian J.* **2017**, *12*, 2033–2037.
[25] V. A. Bragina, A. V. Orlov, S. L. Znoyko, A. V. Pushkarev, D. O. Novichikhin, N. V. Guteneva, M. P. Nikitin, B. G. Gorshkov, P. I. Nikitin, *Anal. Methods* **2021**, *13*, 2424–2433.
[26] J. Shen, Y. Zhou, F. Fu, H. Xu, J. Lv, Y. Xiong, A. Wang, *Talanta* **2015**, *142*, 145–149.
[27] I. Martiskainen, S. M. Talha, K. Vuorenpää, T. Salminen, E. Juntunen, S. Chattopadhyay, D. Kumar, T. Vuorinen, K. Pettersson, N. Khanna, G. Batra, *Anal. Bioanal. Chem.* **2021**, *413*, 967–978.
[28] X. Xia, Y. Xu, X. Zhao, Q. Li, *Clin. Chem.* **2009**, *55*, 179–182.
[29] B. G. An, H. R. Kim, M. J. Kang, J. G. Park, Y. W. Chang, J. C. Pyun, *Anal. Chim. Acta* **2016**, *927*, 99–106.

Author Contributions

Vasily G. Panferov conceptualized and implemented the project and wrote the manuscript. Nikita A. Ivanov provided technical ideas and contributed to experimental investigation. Tony Mazzulli, Davor Brinc, and Vathany Kulasingam validated the results. Sergey N. Krylov conceived and guiding the project and wrote the manuscript. All authors reviewed and approved the manuscript.

Data availability statement

The data that support the findings of this study are openly available in "figshare" at https://doi.org/10.6084/m9.figshare.20124224.v1